

~~CONFIDENTIAL~~Copy
RM L53G16

NACA RM L53G16

NACA**RESEARCH MEMORANDUM**

EXPERIMENTAL INVESTIGATION OF AN AXIAL-FLOW SUPERSONIC

COMPRESSOR HAVING ROUNDED LEADING-EDGE

BLADES WITH AN 8-PERCENT MEAN

THICKNESS-CHORD RATIO

FOR REFERENCEBy Theodore J. Goldberg, Emanuel Boxer,
and Peter T. Bernot**NOT TO BE TAKEN FROM THIS ROOM**CLASSIFICATION CHANGED
Langley Naval Aeronautical Laboratory
Langley Field, Va.**UNCLASSIFIED***700-2-2-118*
*and R-118**Effective*
July 27, 1957
CLASSIFIED DOCUMENT*207-4-57*

This material contains information affecting the National Defense of the United States within the meaning of the espionage laws, Title 18, U.S.C., Secs. 793 and 794, the transmission or revelation of which in any manner to an unauthorized person is prohibited by law.

**NATIONAL ADVISORY COMMITTEE
FOR AERONAUTICS****WASHINGTON**

December 11, 1953

~~CONFIDENTIAL~~

NATIONAL ADVISORY COMMITTEE FOR AERONAUTICS

RESEARCH MEMORANDUM

EXPERIMENTAL INVESTIGATION OF AN AXIAL-FLOW SUPERSONIC
COMPRESSOR HAVING ROUNDED LEADING-EDGE
BLADES WITH AN 8-PERCENT MEAN
THICKNESS-CHORD RATIOBy Theodore J. Goldberg, Emanuel Boxer,
and Peter T. Bernot

SUMMARY

Supersonic-compressor blade sections having rounded leading edges with an 8-percent mean thickness-chord ratio and a solidity of about 2.5 were incorporated in a 16-inch-diameter rotor and were tested with and without guide vanes. The blades were designed to have a thickness-chord ratio greater than previous sections of this type by altering the geometry of the supersonic portion of the blade sections and by increasing the turning angles.

The compressor was designed for a pressure ratio of 2.6 with an efficiency of 89 percent at an equivalent weight flow of 29 lb/sec of air at the design tip speed of 1600 fps. Because of mechanical difficulties in the test rig, the tests reported herein were made only in Freon-12. The tests covered a range of tip speeds from 515 to 810 fps in Freon-12 (70 percent to 110 percent of design speed) which corresponds to a range from 1130 to 1760 fps in air.

The rotor with guide vanes produced a pressure ratio of 1.84 with an efficiency of 68 percent at a weight flow of 48.4 lb/sec of Freon-12 at the design tip speed of 730 fps. Operating without guide vanes, the rotor produced a pressure ratio of 2.06 with an efficiency of 71.5 percent at a weight flow of 49.8 lb/sec of Freon-12 which, when converted to air values by maintaining the efficiency constant at 71.5 percent, would yield a pressure ratio of 2.18 and a weight flow of 27.5 lb/sec of air. Increasing the thickness-chord ratio for approximately the same solidity results in lower relative total-pressure recovery, apparently a result of the increased boundary-layer separation which is caused by larger turning and greater rate of area growth in the subsonic portion of the passage between blades.

INTRODUCTION

The operation of axial-flow supersonic compressors has been shown both theoretically and empirically to be capable of producing a much greater pressure rise per stage than that of conventional subsonic designs (refs. 1 and 2). Of the several types of supersonic compressors described in reference 1, the one having supersonic relative inlet velocities and deceleration through the speed of sound in the rotor was the subject of the present investigation. Because the use of thin blades introduced difficult structural design problems, the shock-in-rotor type of supersonic compressors tested so far by the National Advisory Committee for Aeronautics were either shrouded or designed to operate in Freon-12 gas which reduces the centrifugal force by a factor of approximately 4. In an effort to increase the practicability of this type of supersonic compressor, the factors leading to increased thickness-chord ratio were analyzed from two-dimensional-flow considerations. It was found that an increased thickness-chord ratio was obtained by increasing the total turning angle, the proportion of turning in the supersonic section of the blade passage, and the rate of area growth in the subsonic portion of the blade passage. In order to evaluate the performance of blade sections having a greater thickness-chord ratio than previous designs of this type (8 percent as compared with 4 percent at the mean radial station reported in ref. 3), a rotor incorporating these thicker blades was designed and constructed to be tested in air.

The rotor was designed to produce a pressure ratio of 2.6 and an efficiency of 89 percent at a tip speed of 1600 fps in air with a weight flow of 29 lb/sec of air. However, because of the inability of the gearbox bearings to withstand the high temperatures obtained at the high rotational speeds, all performance tests had to be made in Freon-12 which permitted testing at about one-half the rotational speed required for air. Tests were, therefore, made through a range of equivalent tip speeds from 515 to 810 fps (70 percent to 110 percent of design speed) in Freon-12. The rotor blades were designed with sharp leading edges but, in the initial stages of testing, these sharp leading edges were damaged because of malfunction of the throttle. Consequently, a radius was machined on the leading edge of each rotor blade. The effects of rounding the leading edges of the blades cannot be fully evaluated until results of tests are obtained for the original sharp leading-edge design. Tests to obtain these data have been initiated.

The present investigation was conducted by the Supersonic Compressor Section of the Compressibility Research Division at the Langley Laboratory.

SYMBOLS

a	velocity of sound, fps
M	Mach number, ratio of flow velocity to velocity of sound, V/a
P	total or stagnation pressure, lb/sq ft
p	static pressure, lb/sq ft
T	total or stagnation temperature, °R
t	static temperature, °R
ΔT	measured stagnation-temperature rise, °R
$\Delta T'$	isentropic stagnation-temperature rise, °R
U	rotational velocity of blade element at any radius, fps
V	velocity of fluid, fps
W	weight flow, lb/sec
β	angle between axial direction and flow direction, deg
δ	ratio of actual inlet total pressure to standard sea-level pressure, $P_0/2116$
γ	ratio of specific heats
η	adiabatic efficiency, $\Delta T'/\Delta T$
θ	ratio of actual inlet stagnation temperature to standard sea-level temperature, $T_0/518.4$
ϕ	turning angle, rotor coordinates, deg
ρ	density, slugs/cu ft
P_4/P_2	relative total-pressure recovery
$W \frac{\sqrt{\theta}}{\delta}$	equivalent weight flow, lb/sec

$U_t/\sqrt{\theta}$ equivalent tip speed, fps

Subscripts:

- a axial
- t tip
- o settling chamber
- 1 rotor entrance, stationary coordinates
- 2 rotor entrance, rotor coordinates
- 4 rotor exit, rotor coordinates
- 5 rotor exit, stationary coordinates

GENERAL AERODYNAMIC DESIGN

Rotor Design Requirements

The general design specifications for the compressor were the same as for those reported in references 2 and 3 and are outlined below:

Tip diameter, in.	16
Hub-tip diameter ratio	0.75
Axial Mach number at entrance to rotor	0.80
Tip speed in air at standard conditions, fps	1600
Prerotation upstream of rotor	Little or none
Mach number leaving rotor	Subsonic

✓ The guide-vane turning distribution was selected to give constant, radial, relative inlet Mach number and total pressure. The rotor was designed for nearly constant radial work input. The turning-angle distribution associated with constant work input results in a decreasing thickness from root to tip because the thickness is a function of the turning angle for a given chord length.

The rotor exit conditions at the mean diameter were obtained with the following assumptions:

- (1) Diffusion to a relative rotor exit Mach number M_4 of 0.75.
- Although previous designs were based on a relative exit Mach number of

0.80, it was felt that better diffusion was possible when based upon results in reference 3 where a relative exit Mach number of 0.70 was obtained although a design value of 0.80 was used.

(2) Relative total-pressure loss equal to that through a normal shock at the entrance Mach number relative to the blades.

(3) A rotor turning angle of 16° .

The turning angles at the tip and root sections were then selected to satisfy the rotor exit Mach number condition, hold the exit total-pressure variation to a minimum, and maintain simple radial equilibrium at the exit of the rotor.

Velocity diagrams for this design are presented in figure 1(a) for air. The expected mean values of total-pressure ratio, efficiency, and weight flow are 2.6, 89 percent, and 29 lb/sec of air, respectively. Because all tests were made in Freon-12, the velocity diagrams for air have been converted to estimated Freon-12 values and are presented in figure 1(b). This conversion produced mean values of total-pressure ratio, efficiency, and weight flow of 2.66, 89 percent, and 54 lb/sec of Freon-12, respectively.

Blade-Section Design

The design method of the blade sections was basically similar to that reported in reference 3. However, in order to obtain thicker blade sections, some modifications were made. These modifications primarily consisted of introducing expansion waves (B to C, fig. 2) downstream of the entrance region, as contrasted with the use of compression waves in reference 3, and completing as much of the turning as possible supersonically in order to increase the thickness of the leading-edge region and reduce the possibility of separation generally associated with a large rate of turning in the subsonic portion. In order to obtain a thickness-chord ratio on the order of 8 percent, the solidity was limited to about 2.5.

APPARATUS AND METHODS

Test Apparatus

The supersonic-compressor test stand was designed in accordance with NACA standards (ref. 4). A sectional view of the test rig is shown in figure 3 and a photograph of the setup appears in figure 4. Uniform,

low-turbulence flow at the rotor is ensured through the use of three 100-mesh screens just ahead of the settling chamber in conjunction with an area reduction of 20 to 1 from the cylindrical settling chamber to the annular test section. Downstream of the rotor the fluid is diffused by a radial, vaneless diffuser. Two aircraft-type radiators are used to remove the heat from the circulating fluid. A drum-type throttle valve with a butterfly vane on the upstream face is used to control the exit pressure. The throttle consists of two concentric perforated cylinders, the inner stationary and the outer rotated by an electric actuator. The butterfly valve is geared to the outer cylinder so that it is closed when the concentric holes are about half closed. This condition produces very sensitive throttle control. A calibrated Venturi tube is incorporated between the throttle and settling chamber. A honeycomb grid composed of cells measuring $1\frac{1}{2}$ by $1\frac{1}{2}$ by 7 inches having a 60-mesh screen at both ends is used just before the Venturi tube to reduce the turbulence and swirl of the fluid entering the tube.

The rotor was driven by a 1,000-horsepower induction motor incorporating a magnetic coupling device for speed control. A three-shaft gear box having a ratio of 15 to 1 was used to increase the rotational speed to a maximum value of 26,000 rpm.

Test Compressor

The rotor was designed to have 46 blades and a rotor hub width of $2\frac{1}{32}$ inches. Two-dimensional blade sections were laid out for each of the three radial stations. The resulting rotor blade sections have thickness-chord ratios of 9 percent at hub, 8 percent at pitch, and 5 percent at tip based upon chord length of sharp leading-edge blades. The ordinates of the three sections are presented in table I. The rotor disk was machined from 14S-T aluminum-alloy forging and the rotor blades from 75S-T aluminum-alloy bar stock. The blades were held in the rotor by a fir-tree method of attachment and were wire-locked in place. A minimum tip clearance of 0.015 inch under static conditions was maintained for all tests.

The guide vanes, which were cast from tin-bismuth, were located upstream of the rotor between an annulus of constant inner and outer radii whose area was $14\frac{1}{4}$ percent greater than that immediately ahead of the rotor in order to reduce the possibility of choking the flow at the vanes. Twenty guide vanes, having a solidity of 1.5, were used. The guide-vane details are presented in figure 5. Downstream stators were not employed.

During preliminary runs in air, strain gages were mounted on four rotor blades to determine the vibratory stress. The strain gages were located at the point of maximum strain as determined by a previous bench test using a tuned column of compressed air to drive a fixed blade. In a preliminary rotor test, a maximum vibratory stress of about 3,000 lb/sq in. was recorded at a tip speed of 1,600 fps in air. A photograph of the test rotor with strain gages attached appears in figure 6.

During the tests to determine the vibratory stress, malfunction of the throttle caused the tin-bismuth guide vanes to melt and resulted in damage to the sharp leading edges of the rotor blades. Therefore, a leading-edge radius of 0.010 inch, which faired into the original outline of the blade section, was machined on each blade as shown in table I.

Although a speed of 1,600 fps was attained for the strain-gage tests, the gear-box bearings of this installation were unable to withstand the high temperatures associated with the high speeds and, therefore, the test program was carried out in Freon-12.

Instrumentation

The compressor test rig was instrumented as recommended in reference 4. A sectional view and a photograph showing the locations of the instruments in the region of the rotor appear in figures 7 and 8, respectively. Four static-pressure orifices spaced 90° apart in the settling chamber were used to measure the total pressure. Four thermocouples were located in the settling chamber at the area centers of equal areas to determine the entrance stagnation temperature. In order to determine the flow angles entering the rotor, a radial survey behind the guide vanes was made at 80 and 100 percent of design speed with a claw-type yaw instrument.

Flow conditions behind the rotor were determined by means of a calibrated combination pitot-static-yaw survey probe, shielded total-pressure rakes, and shielded total-temperature rakes located approximately 3/4 inch behind the trailing edge of the rotor hub. A photograph of these instruments appears in figure 9. All temperatures were indicated on a commercial-type self-balancing potentiometer. All pressures were measured by a multiple-tube mercury manometer board and were recorded simultaneously by photographing the manometer.

Automatic control valves were used to maintain constant, preset values of settling-chamber pressure and temperature during test runs by controlling the rate of flow of supply Freon-12 and cooling water.

The rotor speed was measured by a commercial stroboscopic tuning-fork controlled instrument.

The velocity of sound in the Freon-12 air mixture was measured by an instrument similar to that described in reference 5. From this measurement the proportions of the gas constituents and the physical characteristics of the mixture were determined.

Testing Procedure

In general, the procedure followed in operating the compressor consisted first of obtaining the desired rotational speed unthrottled and then increasing the back pressure by arbitrary increments until fully throttled. The fully throttled position was determined by gradually increasing the compression ratio and noting the throttle position at which surge occurred. The throttle was then opened completely and the process repeated until a point very near the surge point was reached.

Data were taken at each throttle setting to determine the over-all compressor characteristics with the survey probe held at the mean annular radius to measure the flow parameters at that station. A radial survey of pressures and angles was made only at fully throttled conditions.

Tests of the rotor with and without guide vanes were made over a range of equivalent tip speeds from 515 to 810 fps in Freon-12. The settling-chamber pressures varied from 0.15 atmosphere for high-speed runs to 0.50 atmosphere for low-speed runs with a corresponding variation of Freon-12 purity from about 92 to 96 percent by volume.

Reduction of Data

The rotor characteristics were determined in the following manner:

- (1) The weight flow was measured by a calibrated Venturi tube.
- (2) The total pressure and temperature behind the rotor were determined from an arithmetical average of radial total-pressure and temperature measurements made by the fixed rakes.

For radial survey runs employing the pitot-static-yaw survey probe, the rotor characteristics were determined from mass-weighted measurements as described in appendix B of reference 2. The average values of inlet and outlet mass flow as determined from survey measurements were ordinarily within 2 percent of that measured by the Venturi tube. There were occasional differences of as great as 8 percent, generally with the outlet flow higher than the inlet. All values of weight flow presented are those measured by the Venturi tube. As indicated in reference 3, two methods were used to determine the work input of the rotor, one based upon measured total-temperature rise and the other based upon momentum

change across the rotor. All values of efficiency presented are those based upon temperature-rise measurements. These efficiency values were consistently 1 to 5 percent lower than those obtained from momentum-change measurements.

For comparison purposes, the rotor characteristics were converted to corresponding values for air by assuming the same efficiency in air as that obtained in Freon-12 and similar velocity triangles.

RESULTS AND DISCUSSION

Rotor With Guide Vanes

Over-all performance.- The over-all performance of the rotor operating with guide vanes over a range of equivalent tip speeds from 30 percent below design to 10 percent above design is presented in figure 10 in terms of adiabatic efficiency and equivalent weight flow as functions of total-pressure ratio at constant speeds. At the design tip speed of 730 fps, a total-pressure ratio of 1.84 and an efficiency of 68 percent at a weight flow of 48.4 lb/sec of Freon-12 were measured. At design speed, the mass flow was independent of back pressure (fig. 10(b)) which indicates a started condition. As explained in reference 1, a started condition exists when the velocity in the throat is supersonic so that the flow ahead of the rotor cannot be affected by back pressure until the normal shock is forced upstream through the throat. At speeds above design the weight flow was reduced with increasing back pressure, similar to speeds below design, which is indicative of operation with a strong normal shock ahead of the rotor. Previous shock-in-rotor compressors have always stalled when the normal shock moved out of the rotor-blade passage after once having been started. The blade sections tested herein at speeds above design apparently produce a higher static-pressure rise and higher relative total-pressure recovery when operating with a strong normal shock ahead of the blade sections than when the normal shock is located at the most forward stable position within the blade passage. The movement of the strong normal shock ahead of the blade passage due to a change of back pressure causes a small decrease in mass flow.

Rotor-blade-element performance.- Variation of several rotor parameters at design speed and maximum efficiency are presented in figure 11 as functions of radial position. The estimated curves were obtained by converting the original air design values to Freon-12 by assuming the

same relative entrance and exit Mach numbers and flow angles at the mean radial station and the same relative entrance and discharge angles at the root and tip. (See appendix of ref. 3).

The difference between the values of total-pressure ratio obtained from the survey probe and the fixed rakes (fig. 11(a)) is believed to be due to guide-vane wake interference and is a function of instrument location since measurements taken either entirely out of the wake or entirely in the wake will produce over-all results which are too high or too low, respectively.

Since the effect of guide-vane wake was not realized at the outset of this investigation, only a few arbitrary positions were selected for measurements. In obtaining weighted results, three computations were made: one using measurements from the survey probe, one using faired values obtained from measurements from the fixed rakes, and one using values from an arbitrary curve as a possible maximum total-pressure ratio as indicated by the dashed line in figure 11(a). These results are presented as flagged symbols in figure 10 and show a 5-percent variation in total-pressure ratio and a corresponding 6-percent difference in efficiency between the weighted values. Because of the variation at the design point, not only between the weighted values but also between the weighted and arithmetical values, it is believed that the characteristic curves are not necessarily correct because of insufficient circumferential measurements. However, it was felt that further investigation into guide-vane wake interference was not feasible at this time. For future investigations of this type of rotor with guide vanes, care must be exercised to make pressure measurements at a sufficient number of circumferential positions to obtain valid results.

Although measurements of the flow behind the rotor are questionable, the flow parameters can still be used to indicate the relative magnitude of the blade-section performance. The exit Mach numbers, turning angle, and flow angle leaving rotor agree fairly well with the estimated values only at the mean radius. However, the relative total-pressure recovery P_4/P_2 is lower by about 16 percent at the mean radius than that for a normal shock at the design relative entrance Mach number, thus causing lower than estimated values of total- and static-pressure rise across the rotor.

The flow angles downstream of the guide vanes were from 4° to 11° off design in such a direction as to reduce the relative Mach number and air inlet angle to the rotor. However, the flow angle into the rotor is actually from 1° to 5° greater than that predicted because of lower axial velocity into the rotor, as evidenced by lower than estimated weight flow. Therefore, the rotor is operating at a positive angle of attack, which is defined for supersonic compressors as being the angle between the relative upstream undisturbed flow direction and the entrance surface

(AB in fig. 2). Previous supersonic-rotor test results (refs. 2 and 3) have exhibited the same characteristic of operation with small angle of attack which shows a departure from the two-dimensional analysis of reference 1.

The relative total-pressure recovery, exit Mach number, and elemental mass flow are greatest in the region near the hub. Apparently, the inward flow necessary to maintain simple radial equilibrium near the exit of the passage in effect reduces the rate of diffusion which reduces the extent of the boundary-layer separation normally present in the passage of such rotors and, consequently, results in higher relative total-pressure recovery.

Rotor Without Guide Vanes

Over-all performance.— Since previous results of supersonic rotors (refs. 2 and 3) indicated higher total-pressure ratios and efficiencies without guide vanes, it was decided to test this rotor alone.

The over-all performance of the rotor operating without guide vanes over the same speed range as with guide vanes is presented in figure 12 in terms of adiabatic efficiency and equivalent weight flow as functions of total-pressure ratio at constant speeds. The data for the tip speed of 770 fps are not shown in figure 12(b) in order to prevent confusion in reading the curves. At the design tip speed, a total-pressure ratio of 2.06 and an efficiency of 71.5 percent at a weight flow of 49.8 lb/sec of Freon-12 were measured. However, this maximum total-pressure ratio was not always reached without surge. Occasionally, a discontinuity occurred at a total-pressure ratio of about 1.8 at which point the rotor exhibited the characteristics of surge. A further increase in back pressure usually, but not always, returned the rotor to a smooth operating condition until the stall point was reached. Changing the system pressure and temperature within the operating range of the equipment yielded no reproducible pattern to attribute this phenomenon to a Reynolds number effect. The reason for this discontinuity is not understood and, therefore, no explanation is attempted nor can any prediction be made as to whether it will occur in other rotors. In general, however, the rotor alone exhibited characteristics similar to those with guide vanes, that is, constant mass flow at design speed and at speeds above design decreasing mass flow with increasing back pressure.

Rotor-blade-element performance.— A variation of several rotor parameters at design speed and maximum efficiency is presented in figure 13 as functions of radial position. Good agreement was obtained between rake and survey-probe total-pressure measurements as shown. Since instrument locations were identical for the two series of runs, the poor agreement between the two methods of measuring total pressure behind the rotor

with guide vanes, therefore, is attributed to guide-vane interference effects. The mass-weighted total-pressure ratio across the rotor is in excellent agreement with that obtained by an arithmetical average as shown in figure 12.

The relative total-pressure recovery (fig. 13) is about 9 percent lower than that estimated but 7 percent higher than that obtained with guide vanes for the same relative exit Mach number resulting in higher static and total pressures at the mean radius than were obtained with guide vanes. The relative total-pressure recovery can be seen to be an inverse function of relative inlet Mach number. Thus, the relative total-pressure recovery without guide vanes was higher at the root because of lower inlet Mach number and conversely at the tip with a greater overall variation for the configuration without guide vanes. The relative total-pressure recovery is, in general, lower than that obtained from the unshrouded rotor of reference 3 by about 4 percent at the root to about 12 percent at the tip. Because the inlet Mach numbers and solidity are approximately the same for the two unshrouded rotors operating without guide vanes, the blade sections of greater thickness-chord ratio have poorer relative total-pressure recovery characteristics that are principally due to the increased boundary-layer separation which is caused by the larger turning and the greater rate of area growth in the subsonic section of the blade.

The spanwise variation of flow angle into rotor (fig. 13(c)) is similar to that noted when operating with guide vanes, that is, increasing toward the tip. Because the geometry of the blade is fixed, the spanwise variation of angle of attack is similar for both operating conditions of the rotor. The average angle of attack is greater than that measured with rotors reported in references 2 and 3. This result is attributed to the rounded leading edges of the blades causing a compression-expansion wave pattern to exist upstream of the blades which reduces the mass flow.

The radial variation of the absolute discharge flow parameters is similar to those obtained with guide vanes.

The effect of back pressure upon the compressor characteristics at the mean radial station at design speed is presented in figure 14 as functions of total-pressure ratio. The inlet conditions are independent of throttling as expected. The relative exit Mach number decreases with increasing back pressure in a manner observed in supersonic diffusers as the normal shock in the passage is moved forward; however, the relative total-pressure recovery remains fairly constant which is contrary to usual results of convergent-divergent supersonic diffusers. This condition may, in part, be attributed to the rapid area expansion as evidenced by the average passage, equivalent conical-expansion angle of 7.4° as compared with approximately 3° conventionally used for supersonic

diffusers. In addition, the radial-flow accelerations within the blades act to reduce the relative total-pressure recovery to values less than those measured in conventional diffuser tests.

The diffuser performance of the pitch section as a function of relative inlet Mach number is shown in figure 15. The data were obtained at the maximum total-pressure-ratio condition over the range of speeds tested. The relative total-pressure recovery decreases very rapidly at inlet Mach numbers above 1.4 and the ability to diffuse, as evidenced by the value of the relative exit Mach number, also decreases rapidly at Mach numbers above 1.4.

The rotor characteristics of tests made without guide vanes have been converted to corresponding values for air and are presented in figure 16. At the design tip speed of 1,600 fps, the rotor would produce a total-pressure ratio of 2.18 with an equivalent weight flow of 27.5 lb/sec of air (efficiency assumed to remain constant at 71.5 percent).

CONCLUSIONS

An experimental investigation has been made in Freon-12 of an axial-flow supersonic compressor having rounded leading-edge blades with an 8-percent mean thickness-chord ratio. The following conclusions are drawn:

1. The rotor operating with guide vanes produced a total-pressure ratio of 1.84 with an efficiency of 68 percent at a weight flow of 48.4 lb/sec of Freon-12 at design tip speed.
2. The rotor operating without guide vanes produced a total-pressure ratio of 2.06 with an efficiency of 71.5 percent at a weight flow of 49.8 lb/sec of Freon-12 which, when converted to corresponding values for air, would be 2.18, 71.5, and 27.5, respectively.
3. At speeds above design for both configurations, the mass flow decreased with increasing back pressure which indicated operation with a strong normal shock ahead of the rotor.
4. The relative total-pressure loss was greater than that estimated which was taken to be equal to that across a normal shock for the relative inlet Mach number. Increasing the thickness-chord ratio of rotor blade sections for approximately the same solidity results in lower relative total-pressure recovery. Apparently, this lower total-pressure recovery is due to increased boundary-layer separation which is caused by larger turning angles and by a greater rate of area growth in the subsonic portion of the passages.

5. The results with guide vanes are questionable in that a circumferential variation of total pressure was noted which is attributed to guide-vane wake since good agreement of circumferential total-pressure measurements was obtained without guide vanes.

6. The rotor operated at a greater angle of attack than previous supersonic rotors investigated because of an upstream bow-wave pattern which results from the rounded leading edges of the blades.

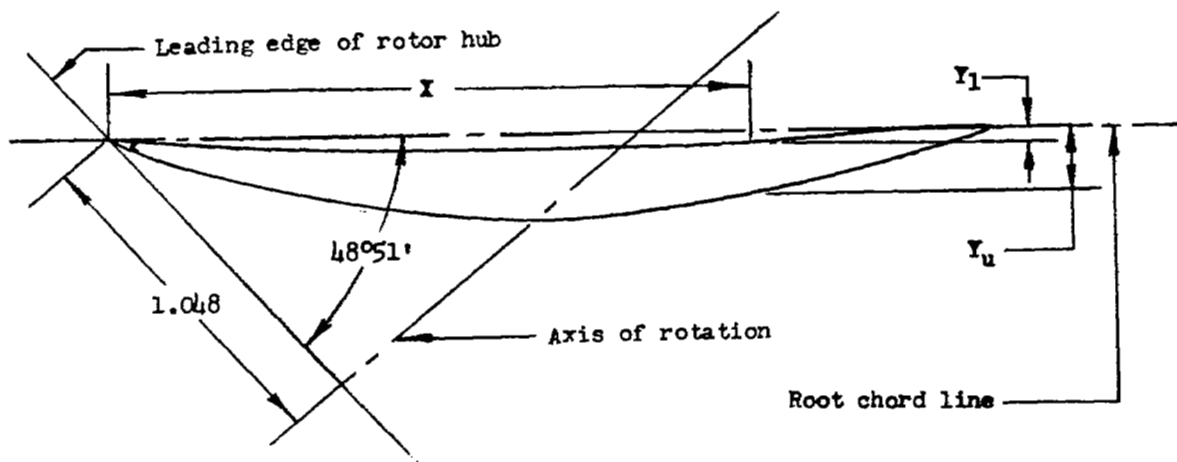
Langley Aeronautical Laboratory,
National Advisory Committee for Aeronautics,
Langley Field, Va., July 7, 1953.

REFERENCES

1. Kantrowitz, Arthur: The Supersonic Axial-Flow Compressor. NACA Rep. 974, 1950. (Supersedes NACA ACR L6D02.)
2. Erwin, John R., Wright, Linwood C., and Kantrowitz, Arthur: Investigation of an Experimental Supersonic Axial-Flow Compressor. NACA RM L6J01b, 1946.
3. Boxer, Emanuel, and Erwin, John R.: Investigation of a Shrouded and an Unshrouded Axial-Flow Supersonic Compressor. NACA RM L50G05, 1950.
4. NACA Subcommittee on Compressors: Standard Procedures for Rating and Testing Multistage Axial-Flow Compressors. NACA TN 1138, 1946.
5. Huber, Paul W., and Kantrowitz, Arthur: A Device for Measuring Sonic Velocity and Compressor Mach Number. NACA TN 1664, 1948.

TABLE I. - BLADE ORDINATES

(a) Root section (6-inch radius).



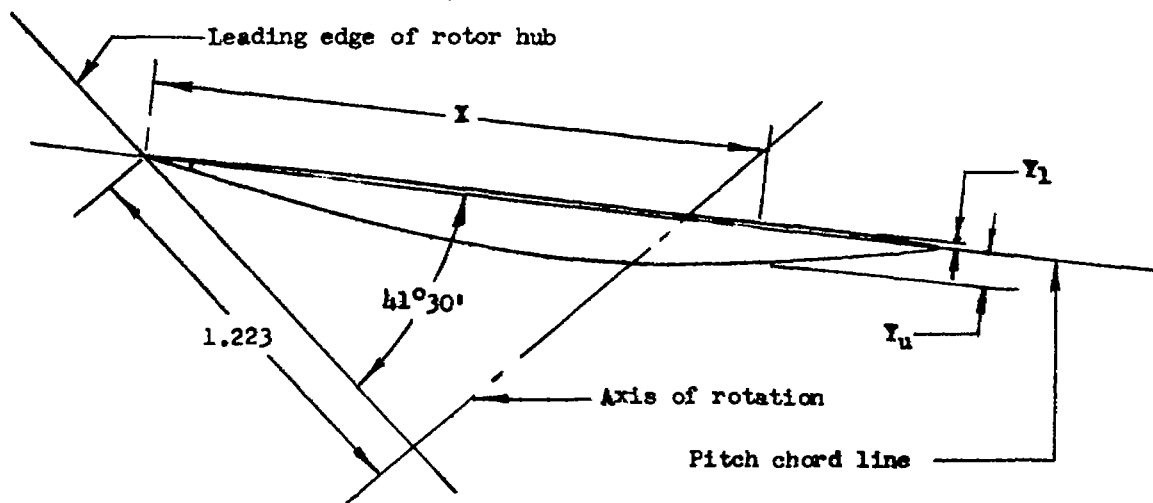
All dimensions in inches

X	Y_u	Y_l
0	0	0
.133	.045	.017
.266	.090	.030
.399	.135	.038
.465	.155	.040
.532	.173	.042
.598	.188	.044
.665	.202	.045
.798	.230	.047
.931	.258	.048
.997	.270	.048
1.063	.273	.049
1.196	.272	.048
1.329	.268	.047
1.396	.263	.047
1.465	.258	.046
1.595	.246	.044
1.728	.228	.041
1.777	.219	.040
1.861	.205	.037
1.994	.180	.033
2.127	.151	.027
2.260	.120	.019
2.393	.085	.009
2.526	.047	.000

NACA

TABLE I. - BLADE ORDINATES - Continued

(b) Pitch section (7-inch radius).



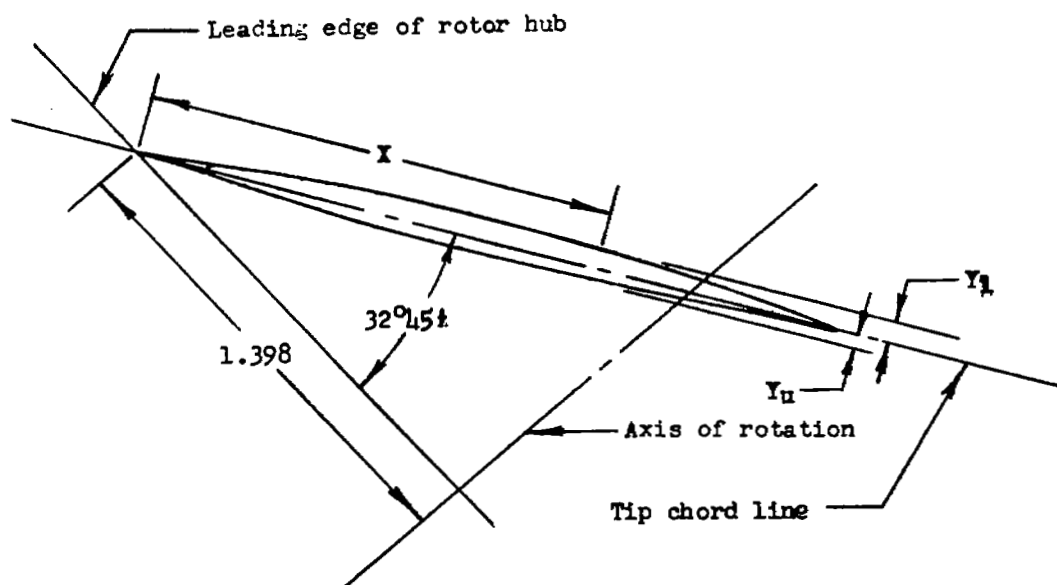
All dimensions in inches

X	Y_u	Y_l
0	0	0
.119	.023	.001
.239	.047	.004
.359	.071	.001
.419	.083	-.003
.478	.095	-.007
.538	.107	-.009
.598	.115	-.011
.718	.127	-.011
.837	.138	-.011
.897	.144	-.011
.957	.150	-.011
1.076	.161	-.011
1.196	.173	-.011
1.256	.175	-.011
1.316	.172	-.011
1.435	.162	-.011
1.555	.151	-.011
1.599	.146	-.011
1.674	.138	-.011
1.794	.122	-.011
1.914	.103	-.011
2.033	.082	-.011
2.153	.058	-.011
2.272	.033	-.011

NACA

TABLE I. - BLADE ORDINATES - Concluded

(c) Tip section (8-inch radius).



All dimensions in inches

X	Y _u	Y _l
0	0	0
.105	.006	-.009
.210	.012	-.018
.315	.017	-.027
.368	.019	-.033
.420	.022	-.039
.473	.024	-.045
.525	.026	-.051
.630	.031	-.059
.735	.036	-.065
.788	.037	-.066
.840	.037	-.067
.945	.037	-.067
1.050	.038	-.067
1.103	.038	-.066
1.155	.038	-.065
1.260	.039	-.063
1.365	.039	-.060
1.404	.039	-.059
1.470	.032	-.057
1.575	.023	-.053
1.680	.015	-.047
1.785	.009	-.041
1.890	.006	-.033
1.995	.004	-.022

NACA

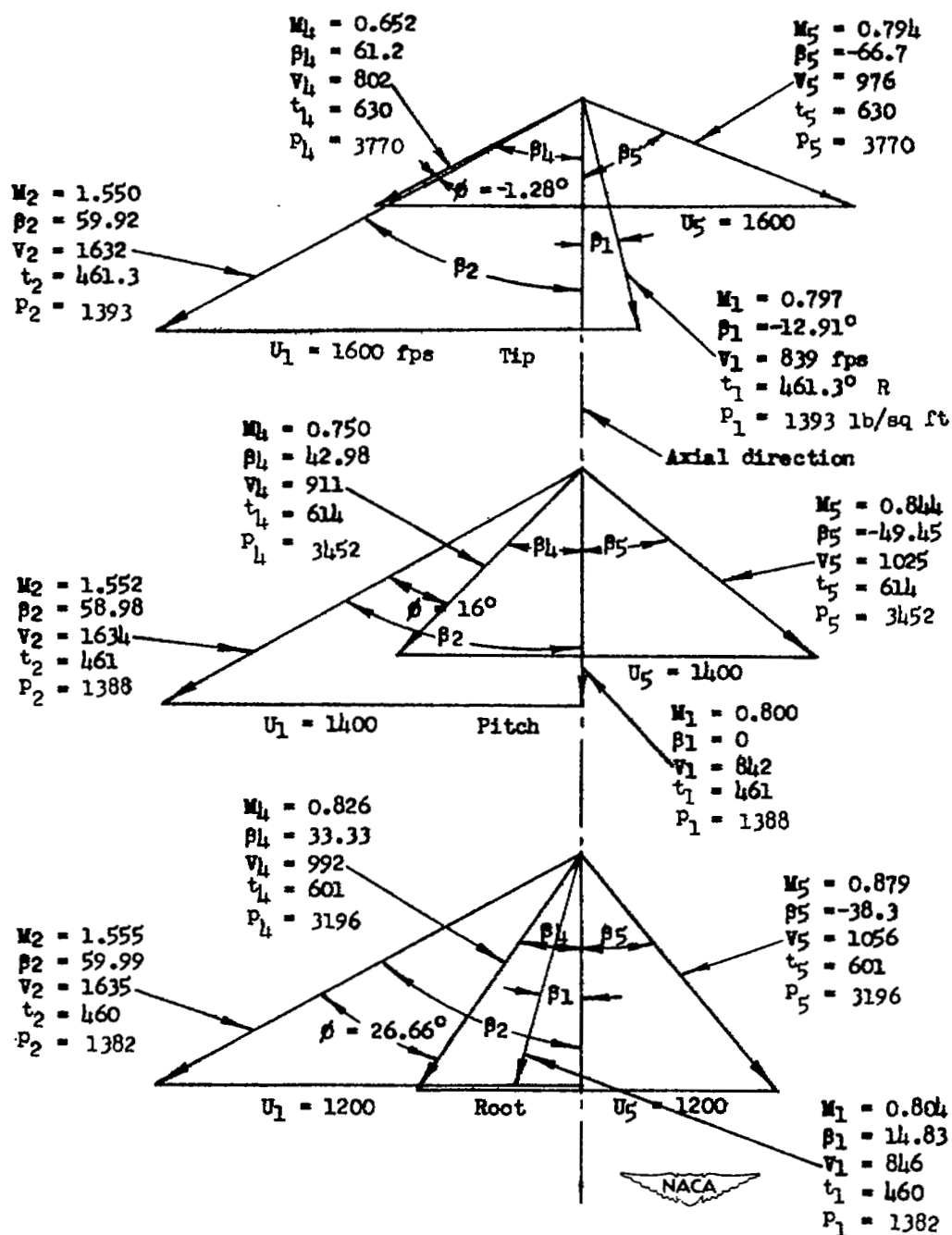
(a) Velocity diagrams for air. $\gamma = 1.4$.

Figure 1.- Supersonic-compressor velocity diagrams for tip, pitch, and root sections. Initial conditions: $P_0 = 2116$ lb/sq ft; $T_0 = 520^\circ$ R.

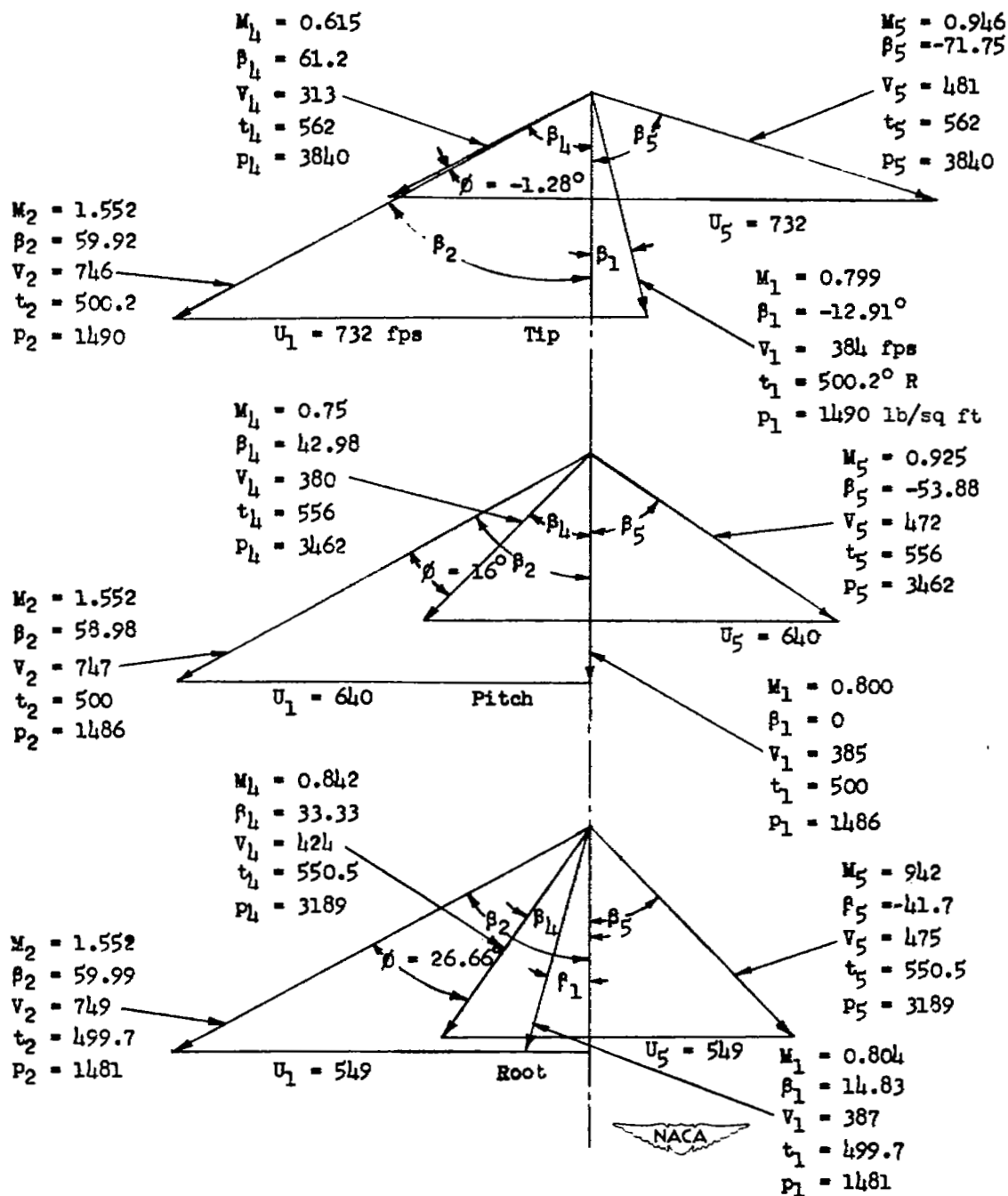
(b) Estimated velocity diagrams for Freon-12. $\gamma = 1.125$.

Figure 1.- Concluded.

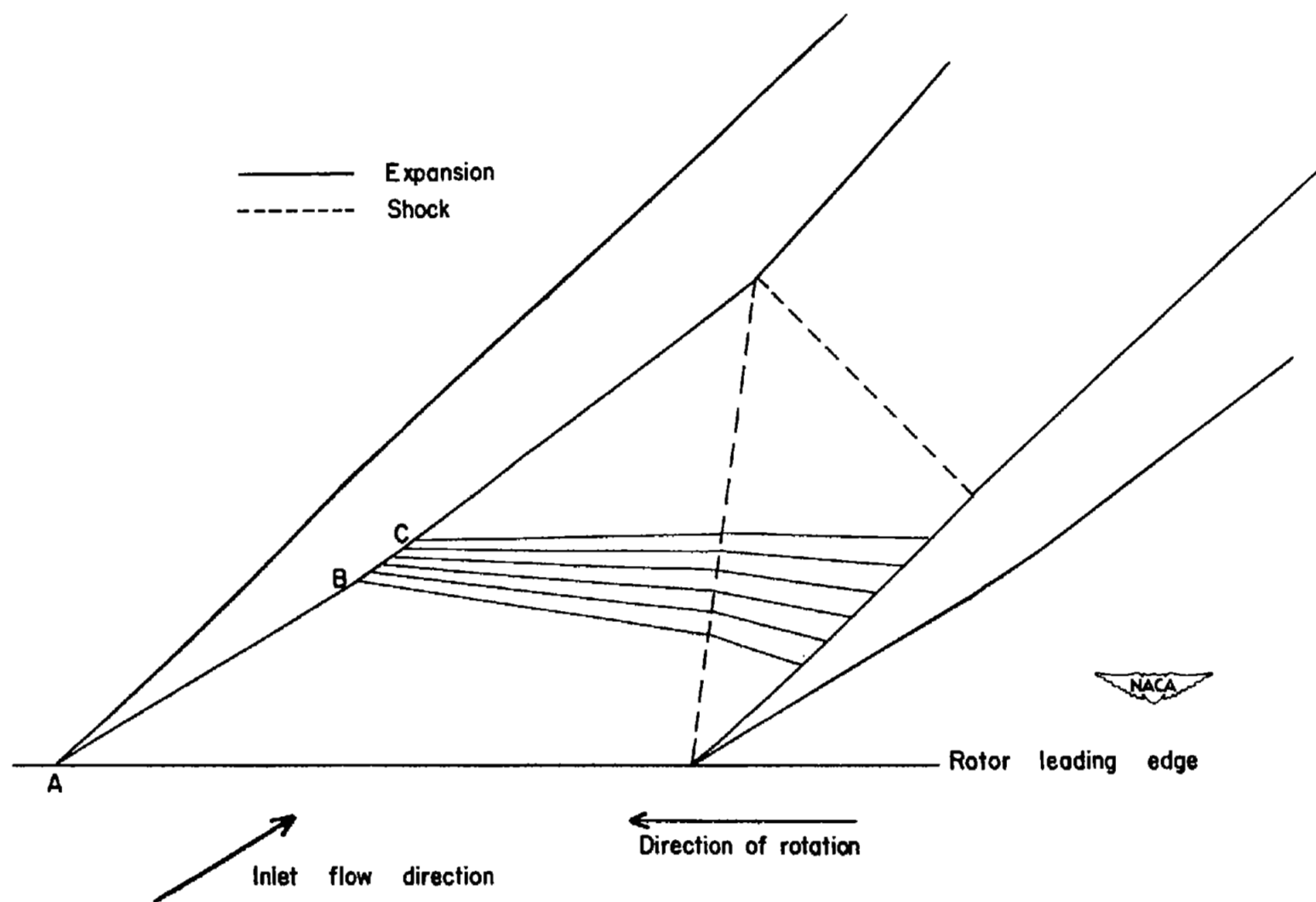


Figure 2.- Supersonic portion of a two-dimensional rotor blade.

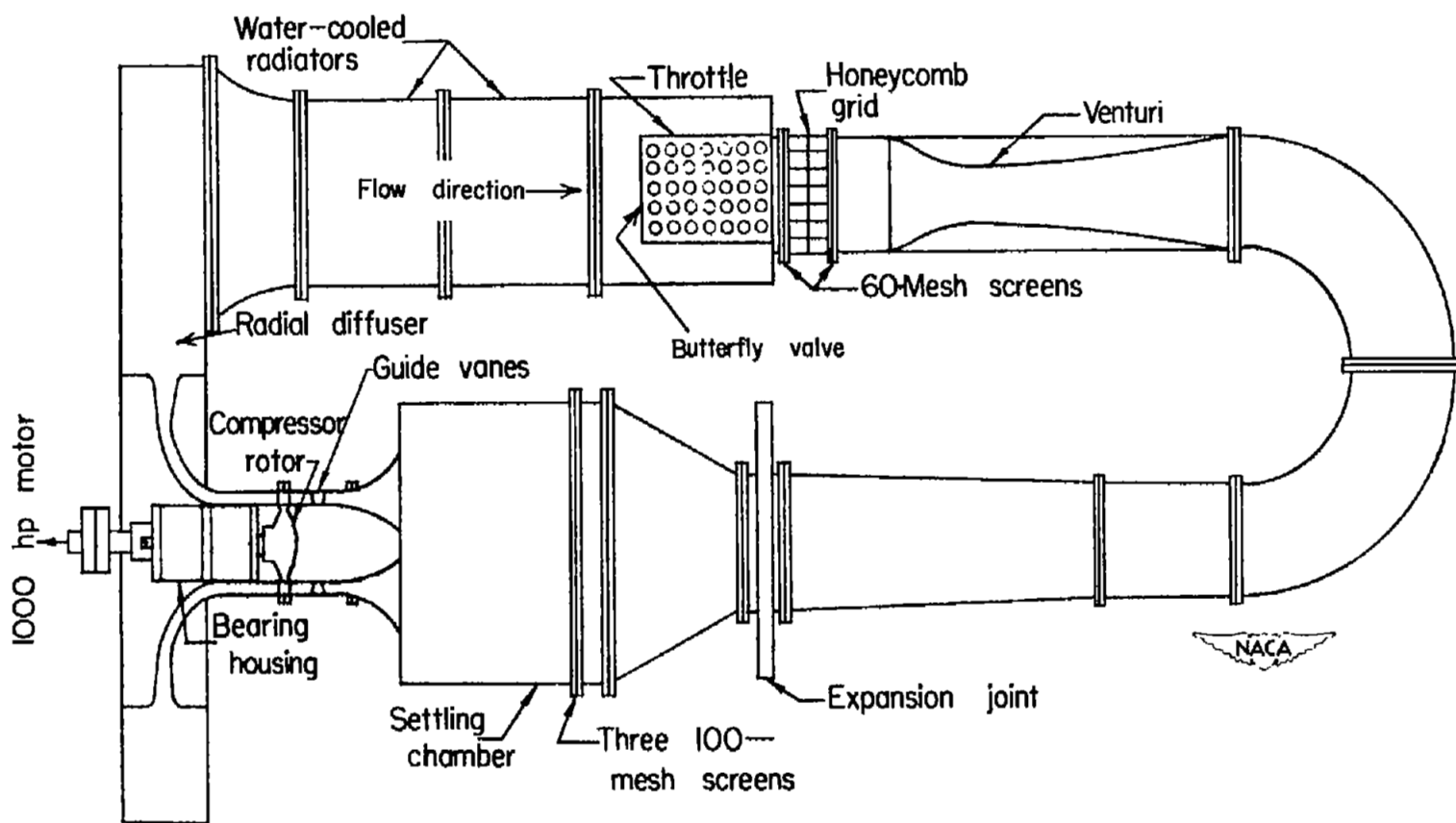
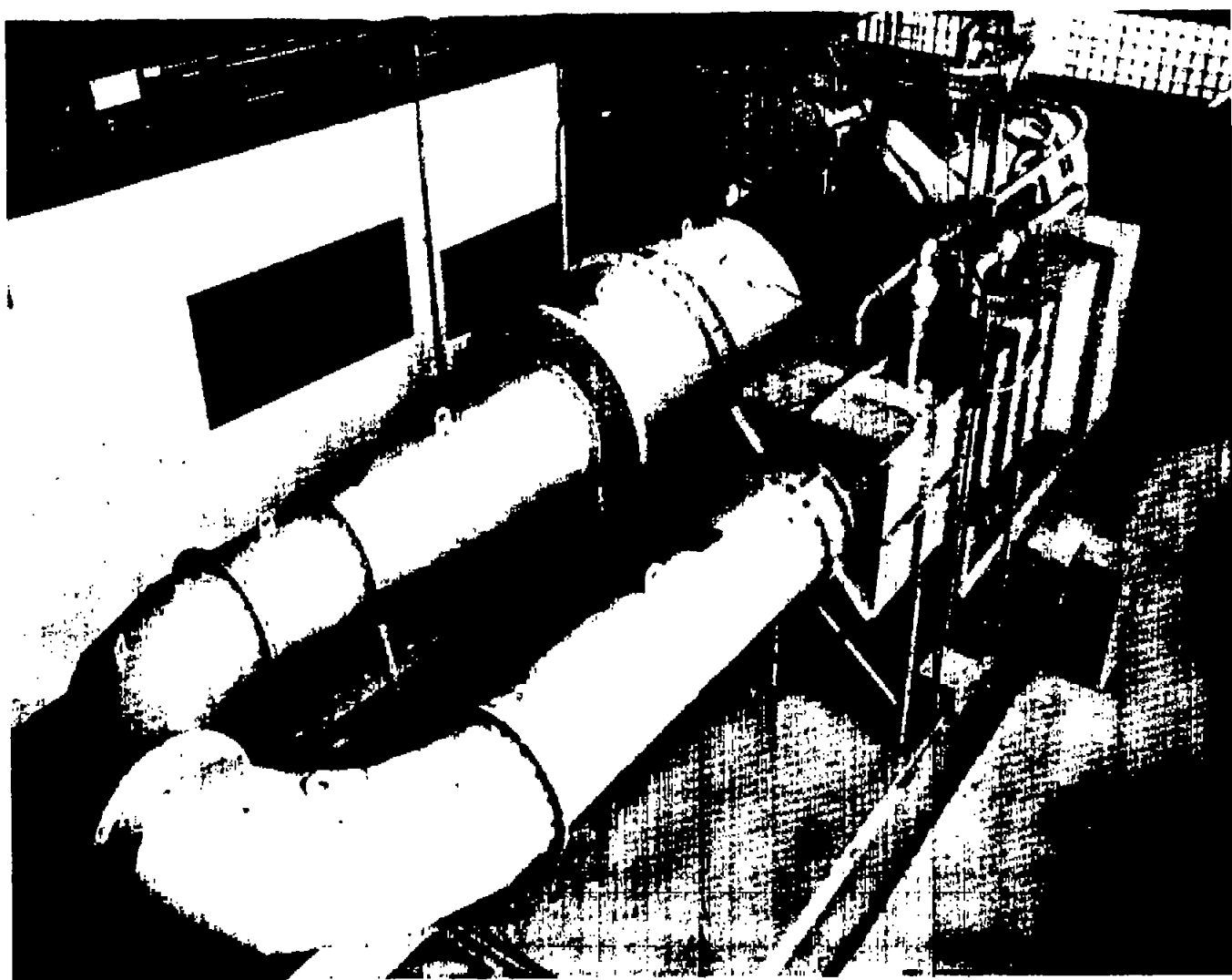


Figure 3.- Arrangement of supersonic-compressor test rig.



L-74608.1

Figure 4.- Supersonic-compressor test rig.

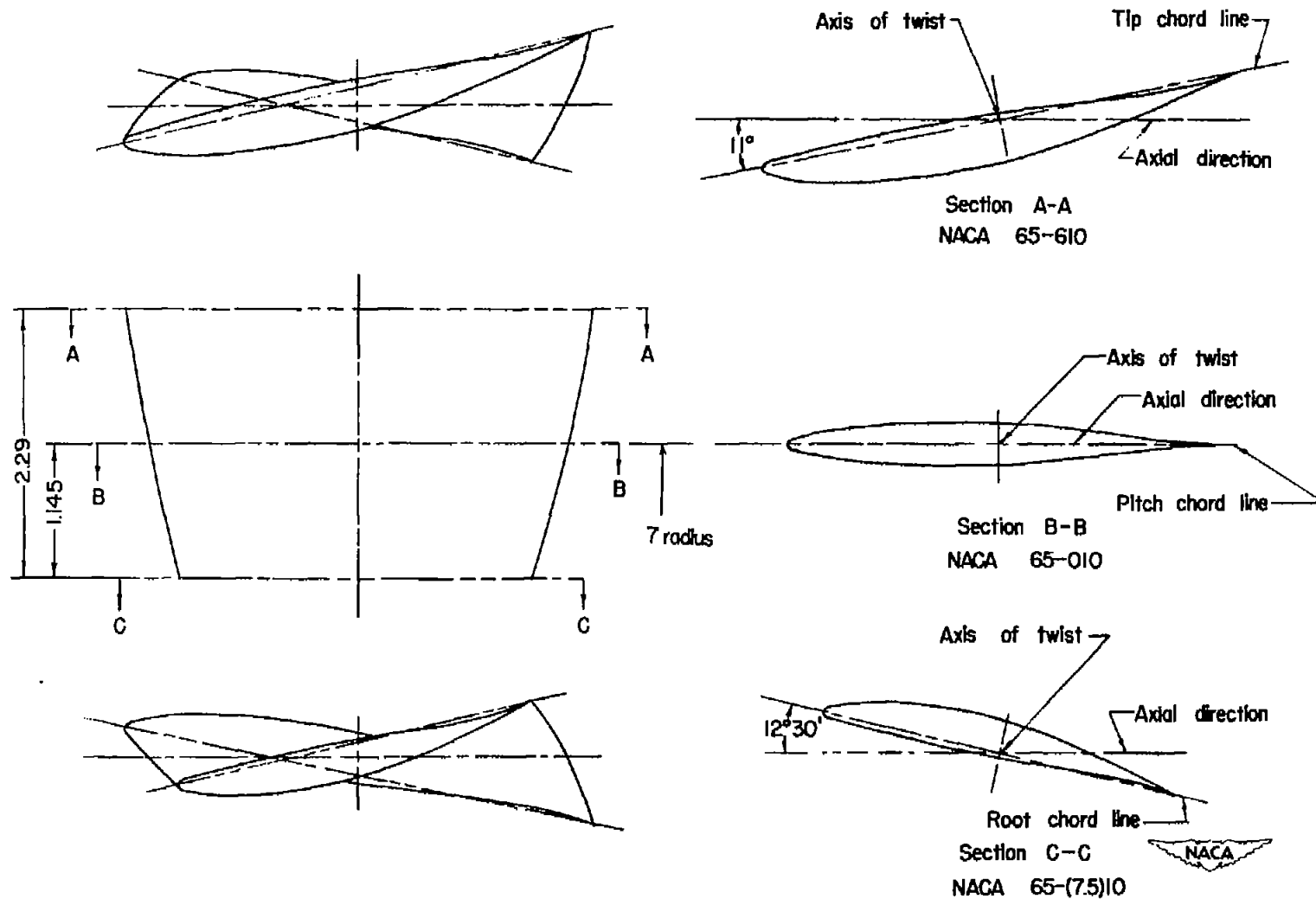


Figure 5.- Guide-vane details. All dimensions are in inches.

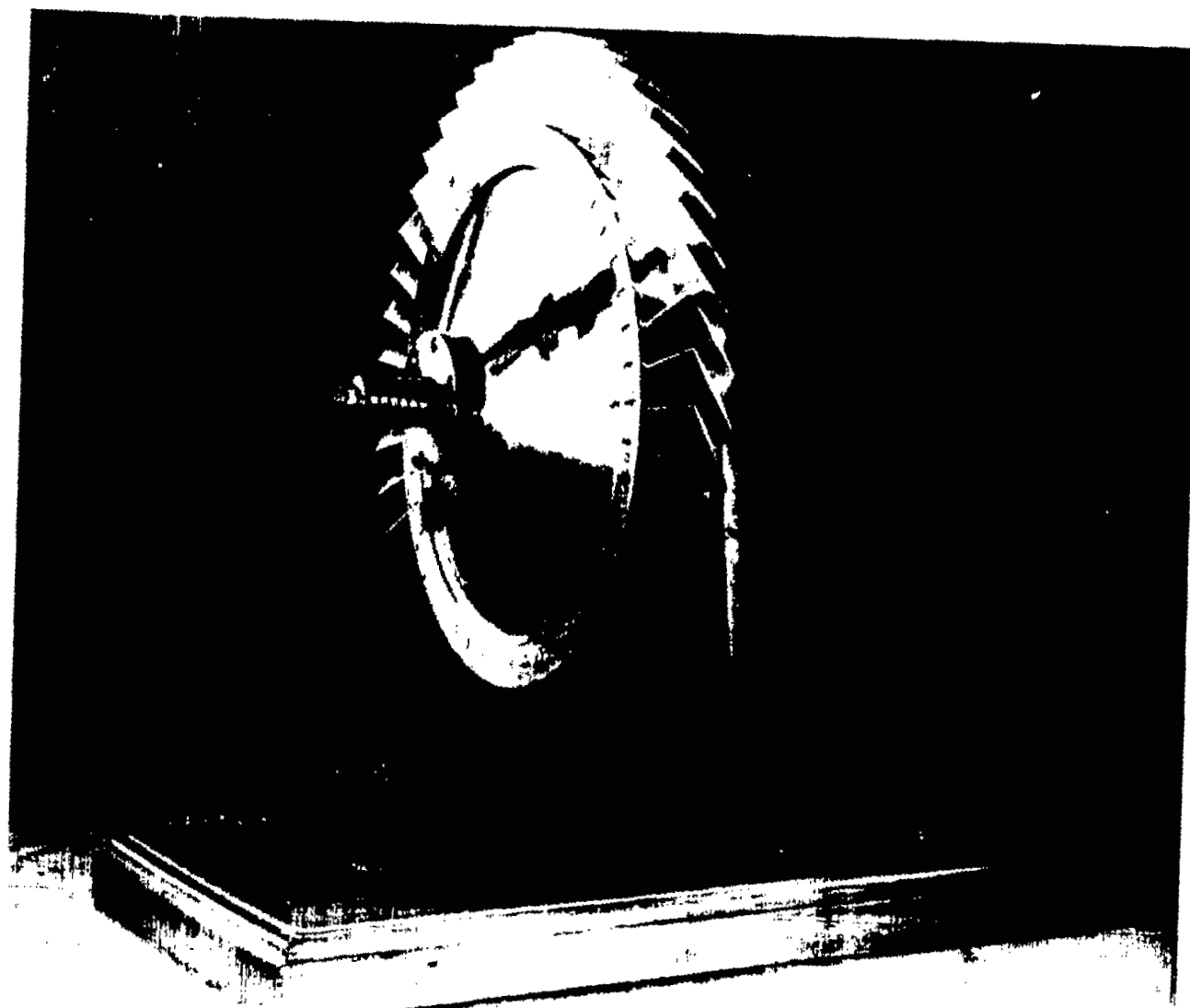


Figure 6.- Test rotor with strain gages attached.

L-63386

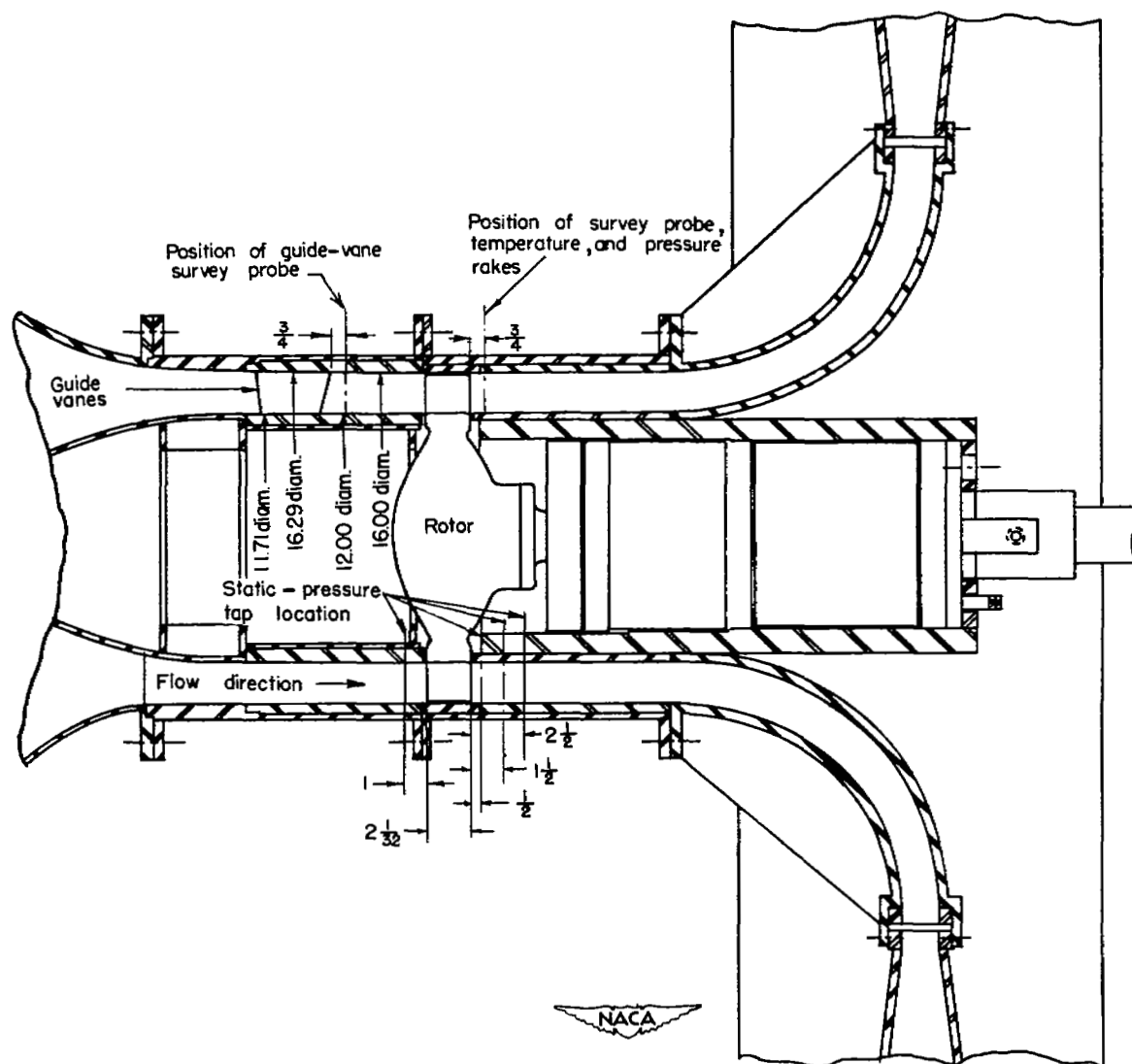
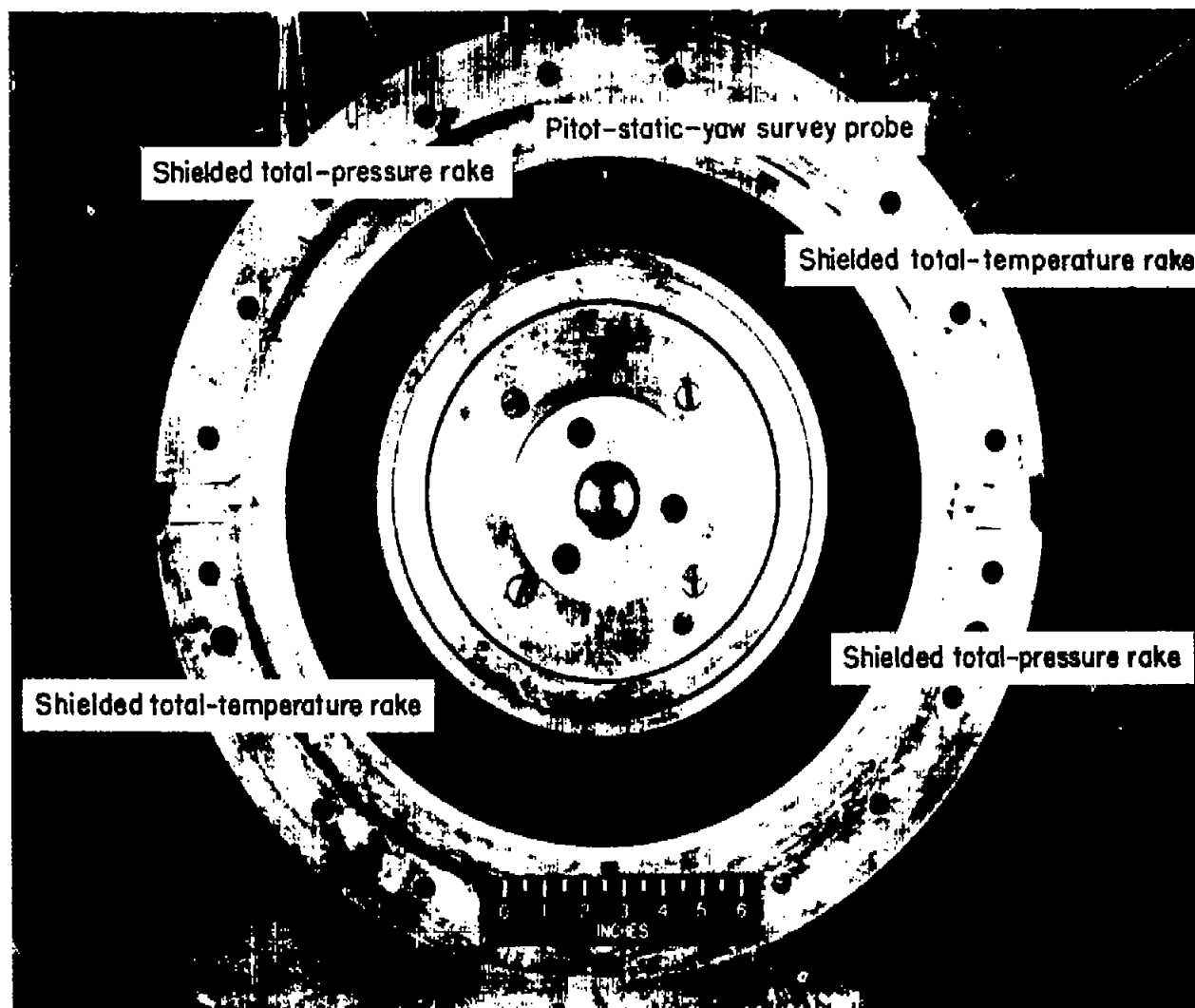


Figure 7.- Sectional view of test section of supersonic-compressor test rig showing location of instrumentation. All dimensions are in inches.



L-74607.1

Figure 8.- Downstream survey probe, total-temperature rakes, and total-pressure rakes.

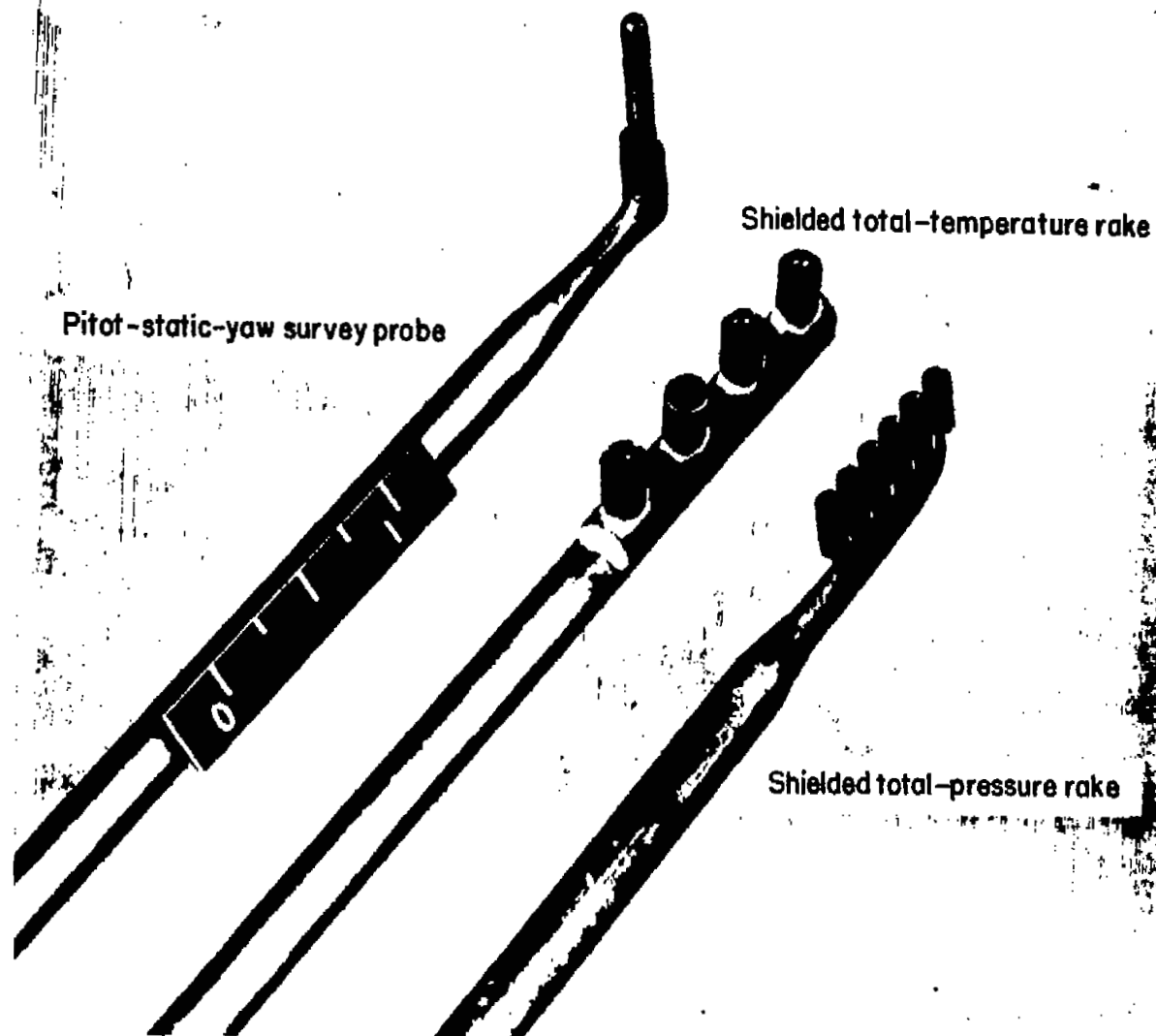
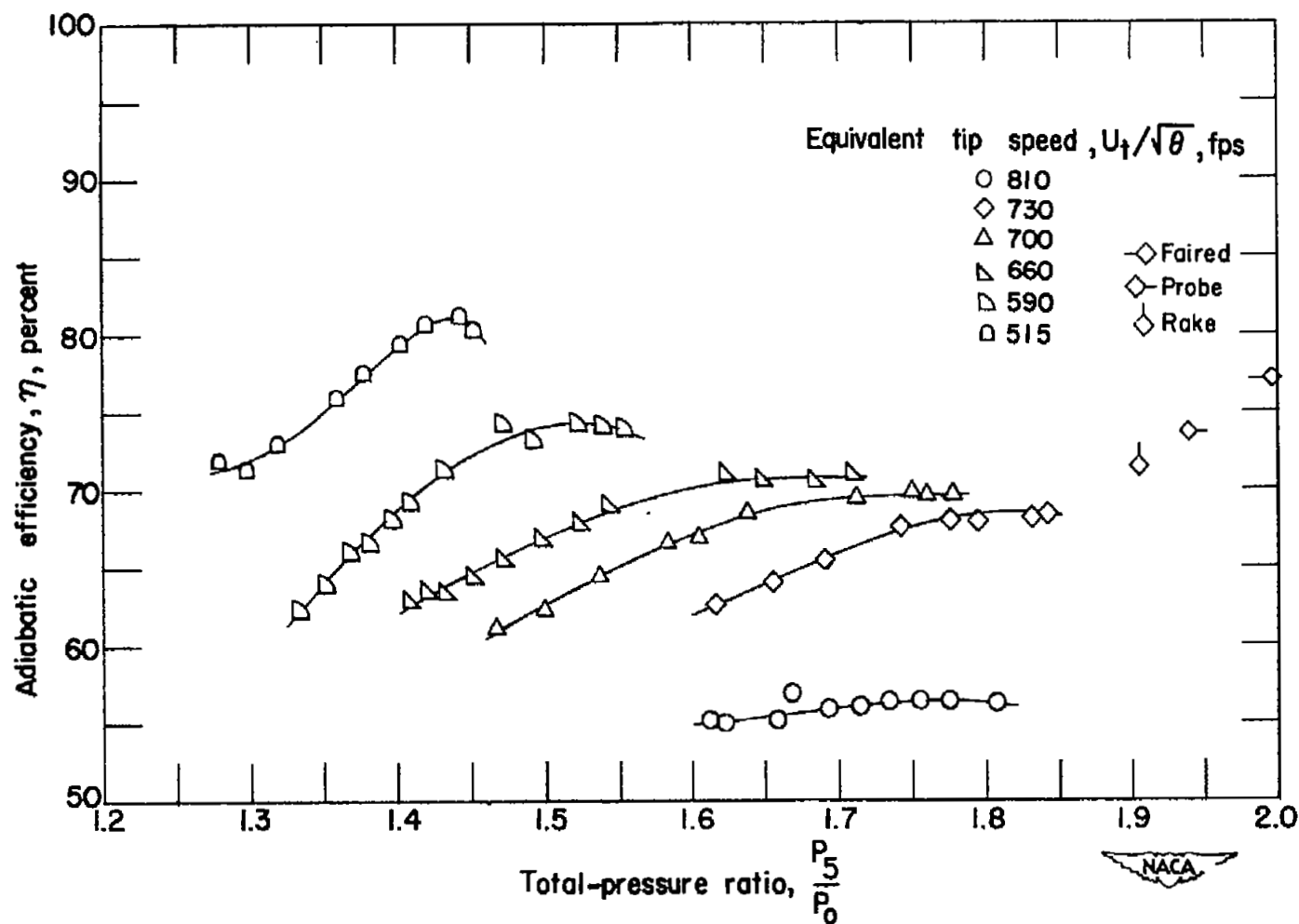


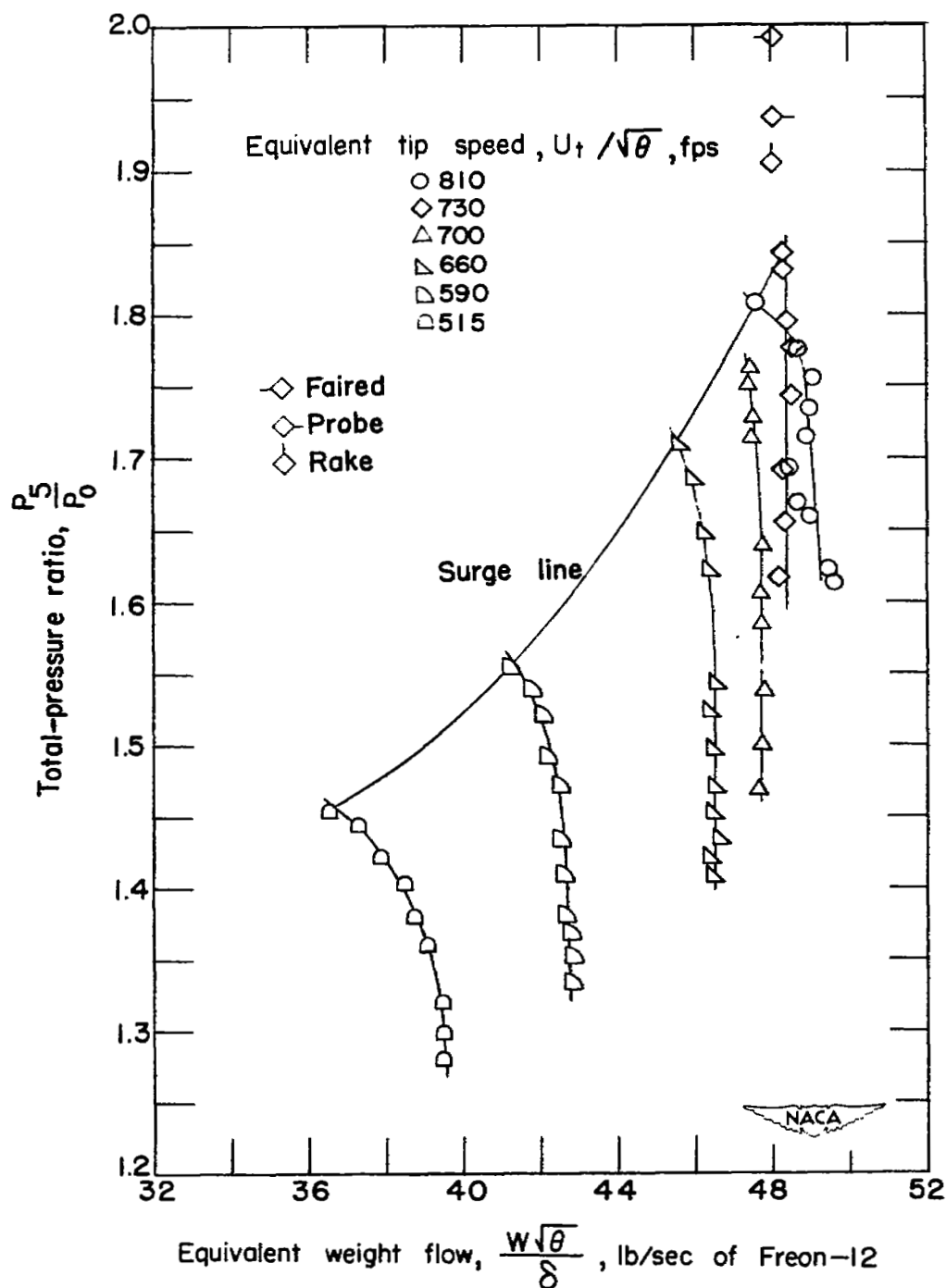
Figure 9.- Detail photograph of flow measuring instruments.

L-77480.1



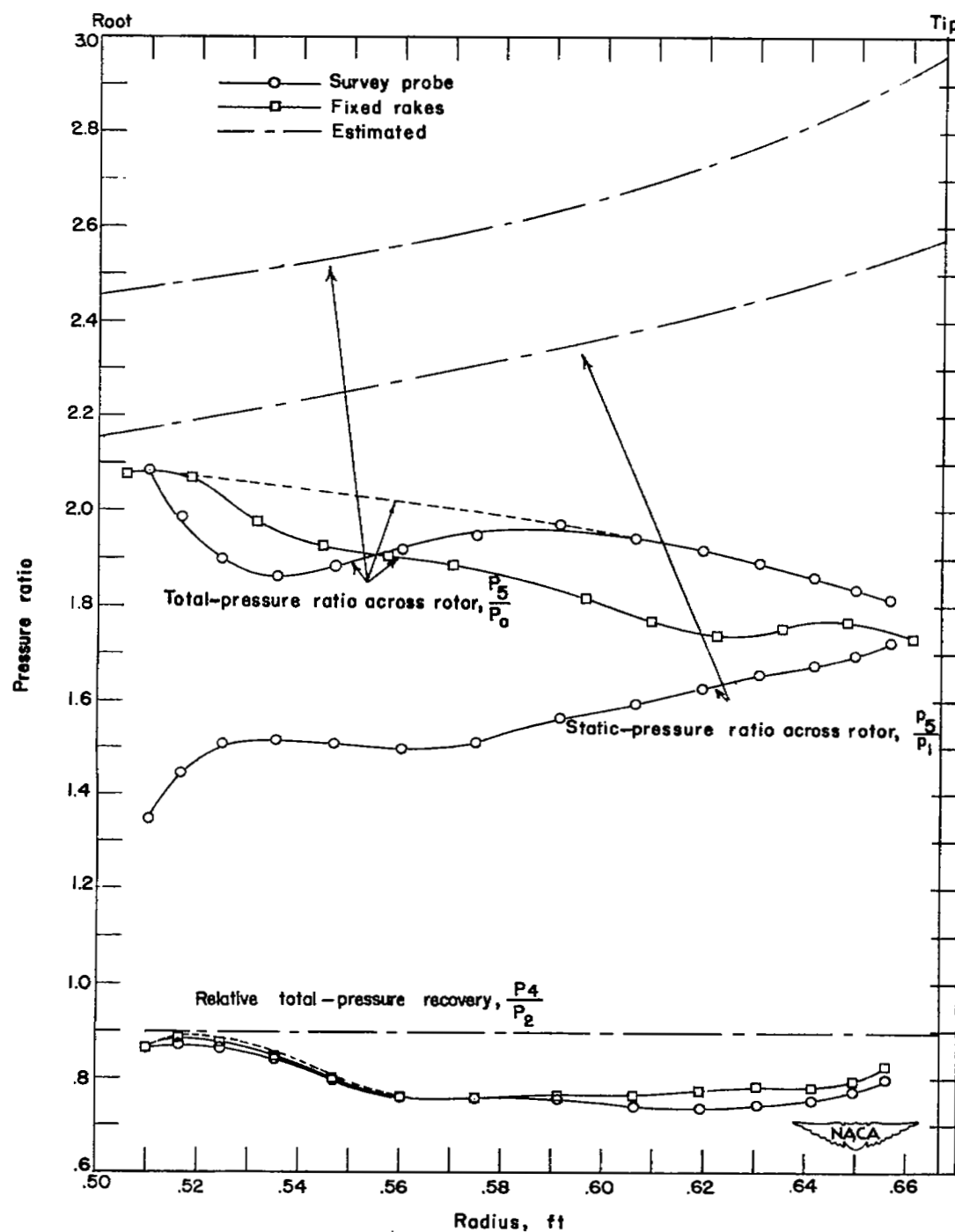
(a) Total-pressure ratio against efficiency.

Figure 10.- Rotor characteristics with guide vanes. Results were obtained in Freon-12. Flagged symbols represent mass-weighted values.



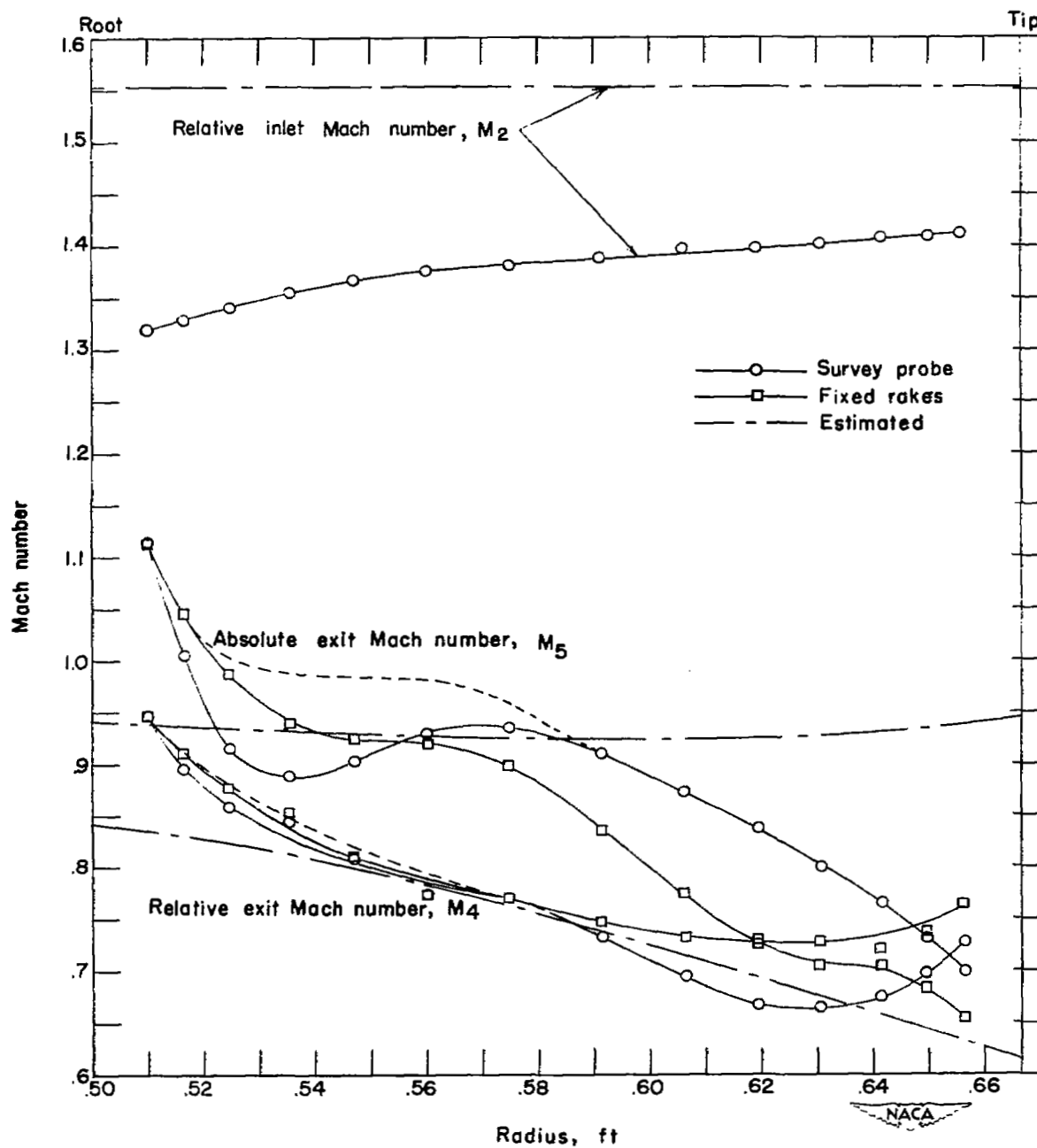
(b) Total-pressure ratio against weight flow.

Figure 10.- Concluded.



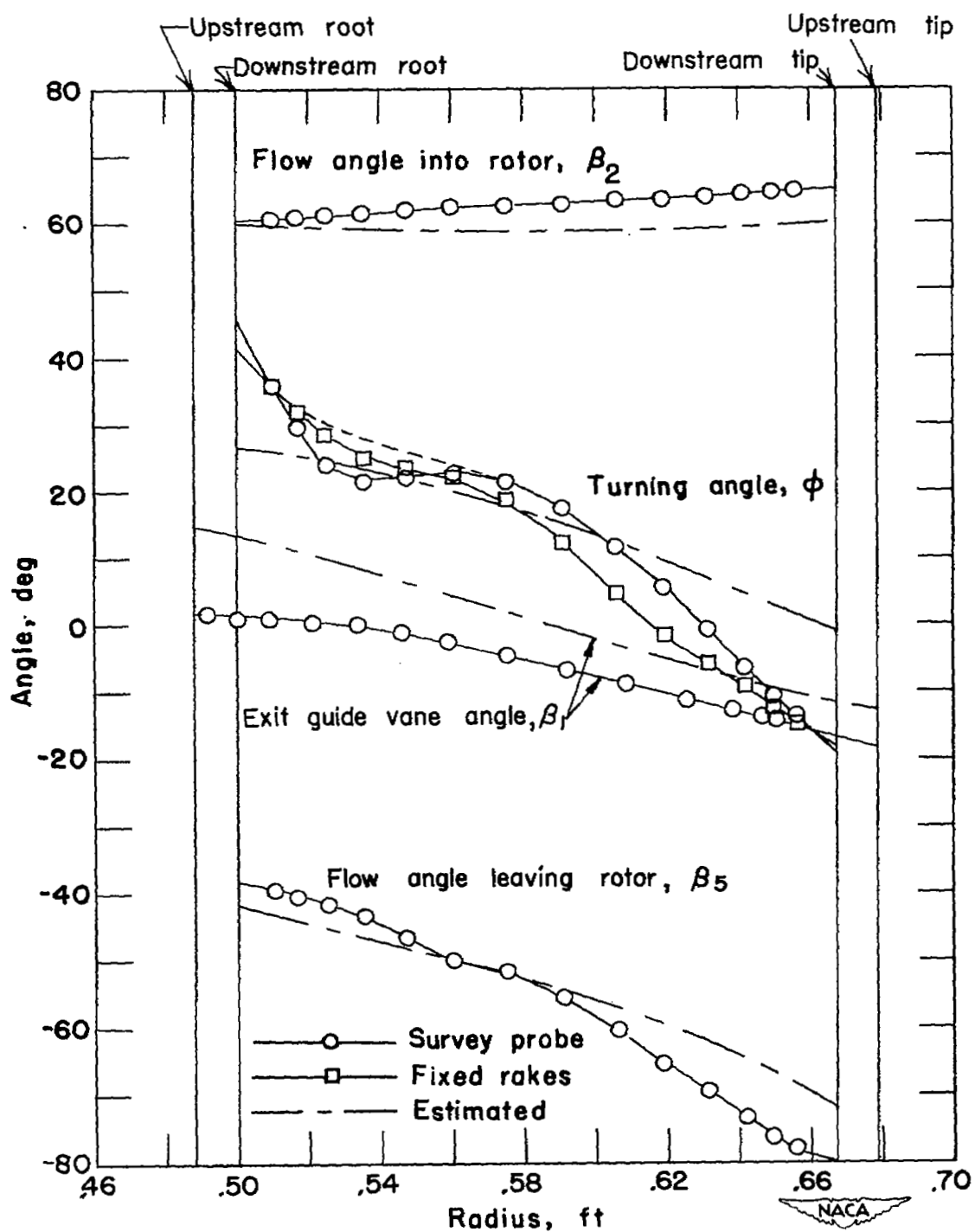
(a) Pressure-ratio distribution.

Figure 11.- Radial variation of compressor parameters at an equivalent design tip speed of 730 fps in Freon-12 with guide vanes.



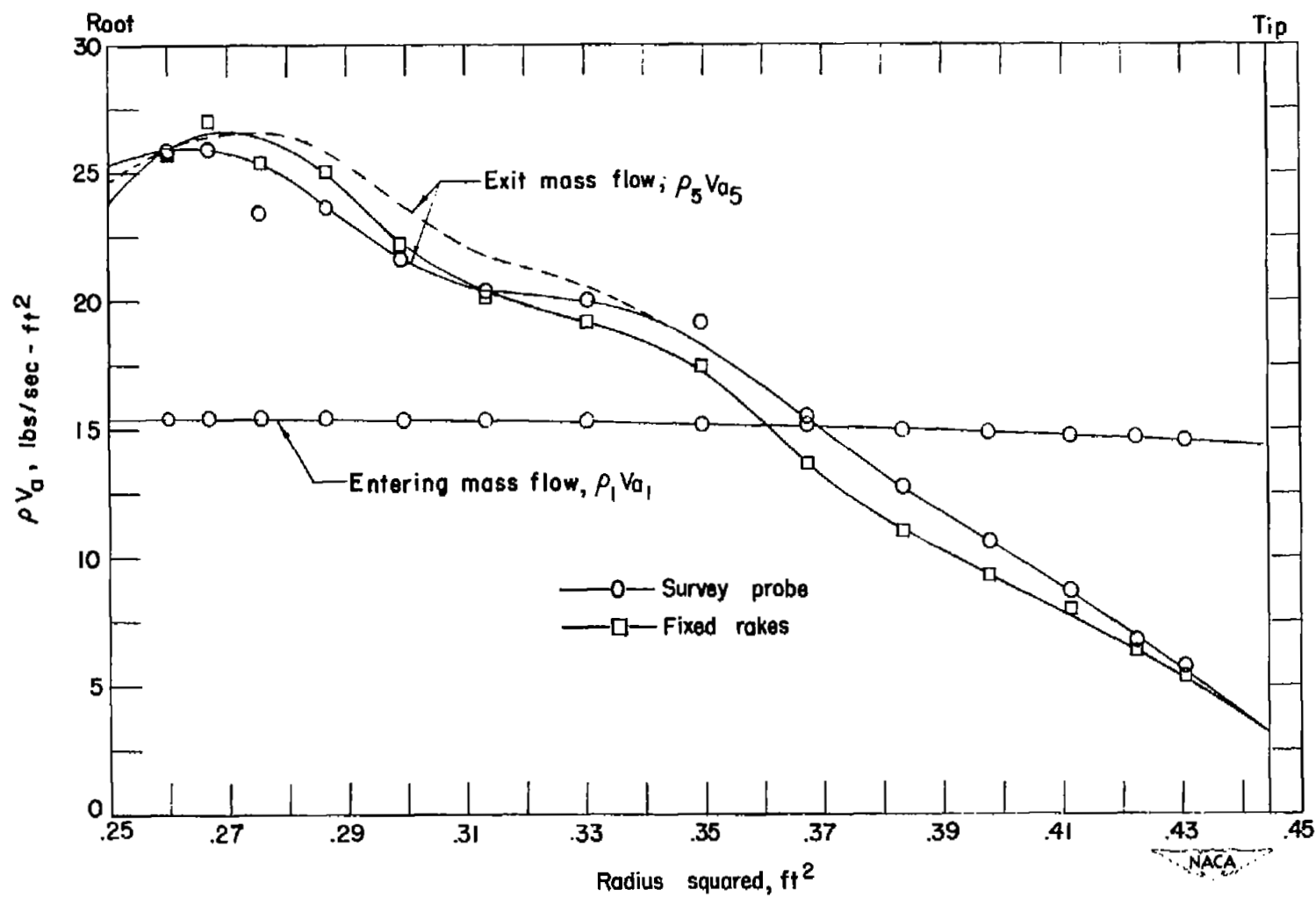
(b) Mach number distributions.

Figure 11.- Continued.



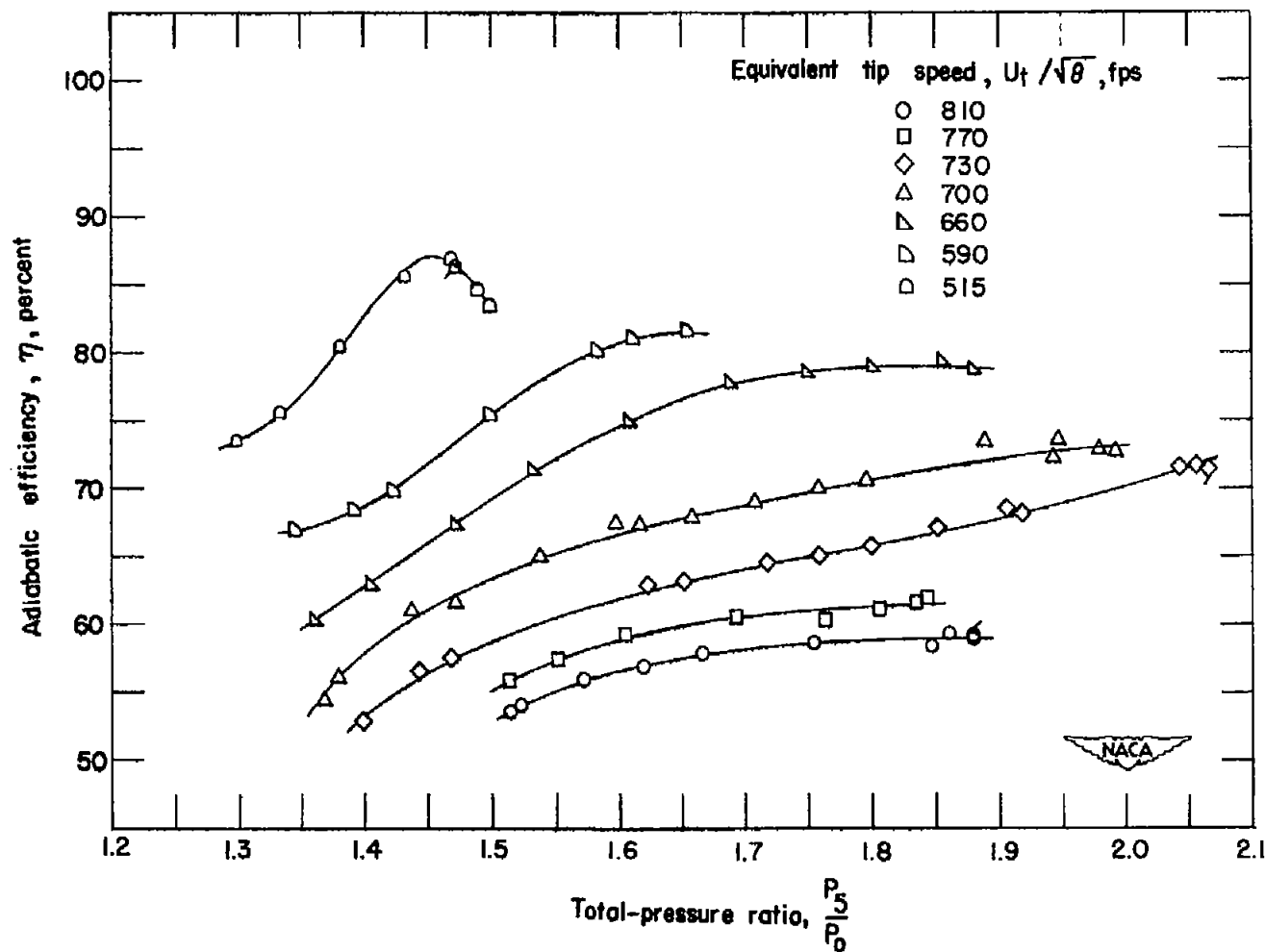
(c) Angle distribution.

Figure 11.- Continued.



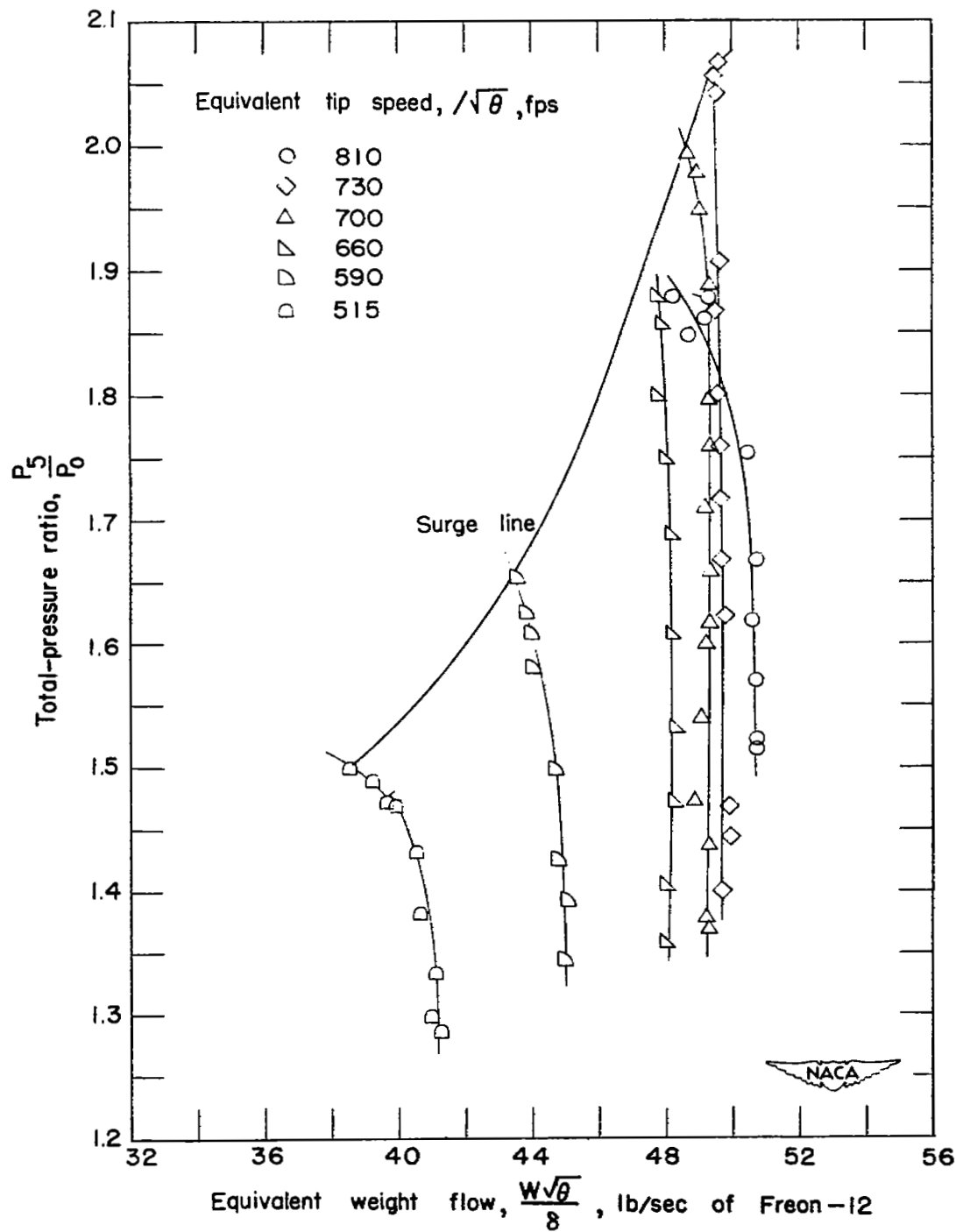
(d) Mass-flow distribution. $P_o = 413.7$ lb/sq ft; $T_o = 520.6^\circ$ R.

Figure 11.- Concluded.



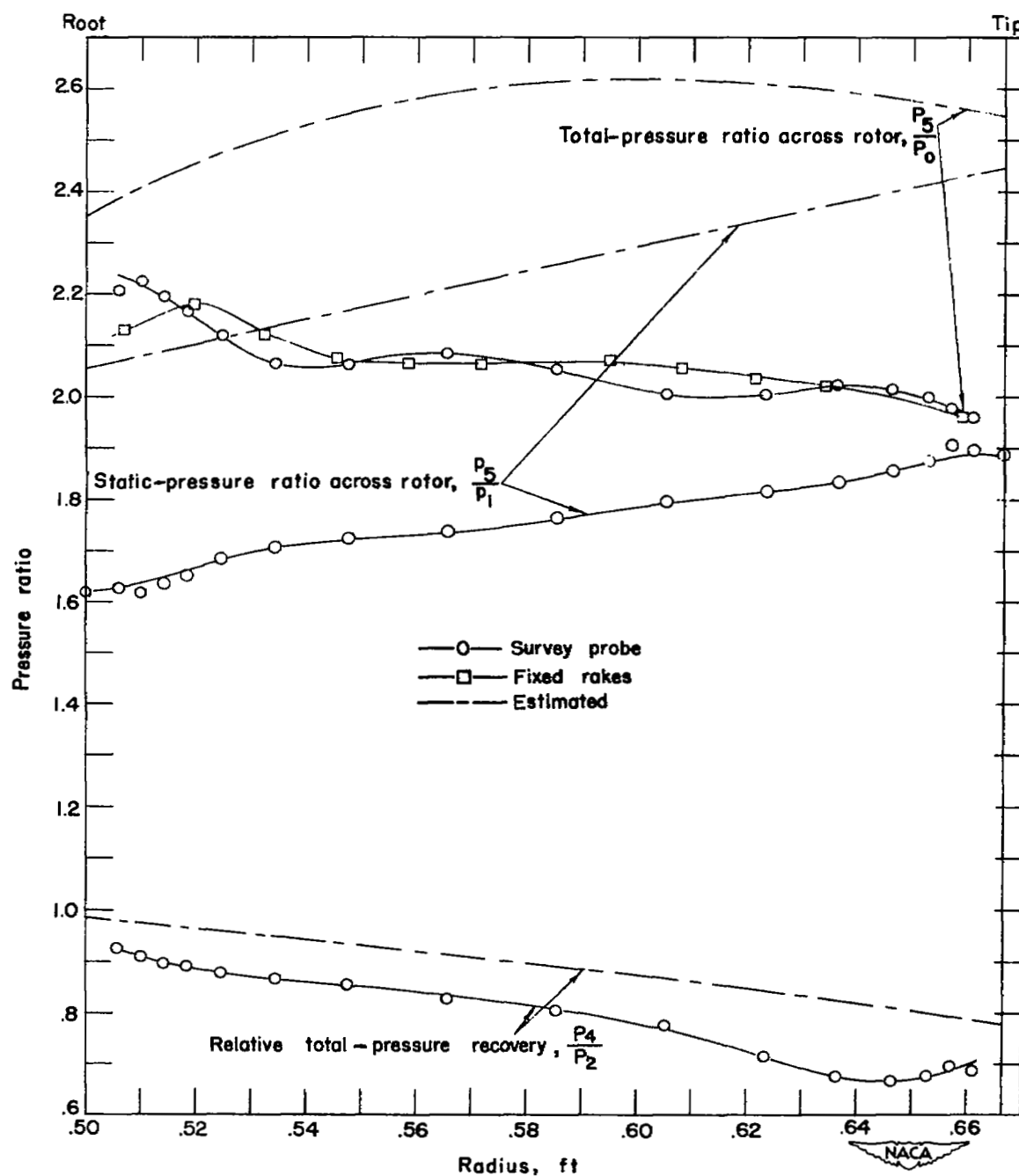
(a) Total-pressure ratio against efficiency.

Figure 12.- Rotor characteristics without guide vanes. Results were obtained in Freon-12. Flagged symbols represent mass-weighted values.



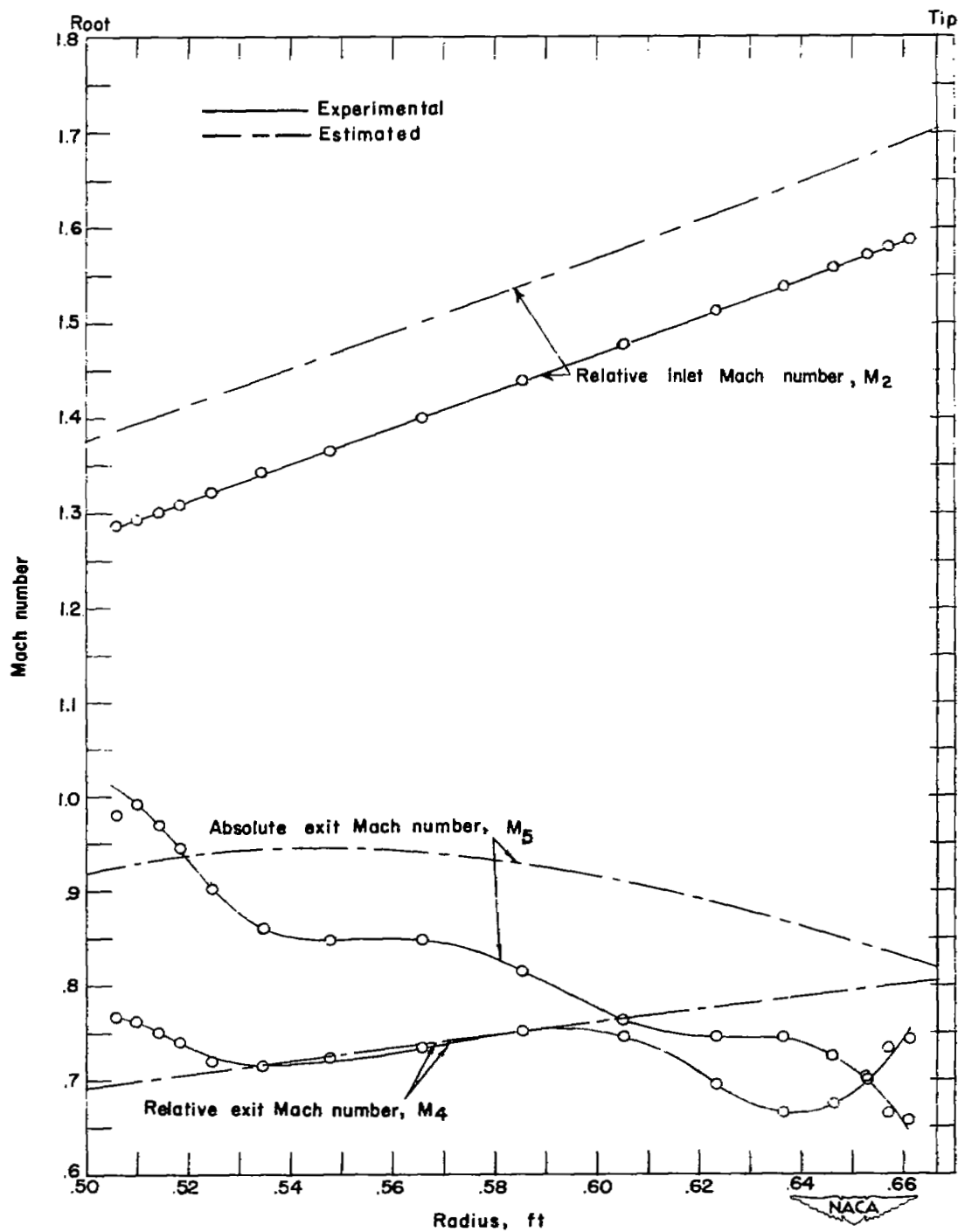
(b) Total-pressure ratio against weight flow.

Figure 12.- Concluded.



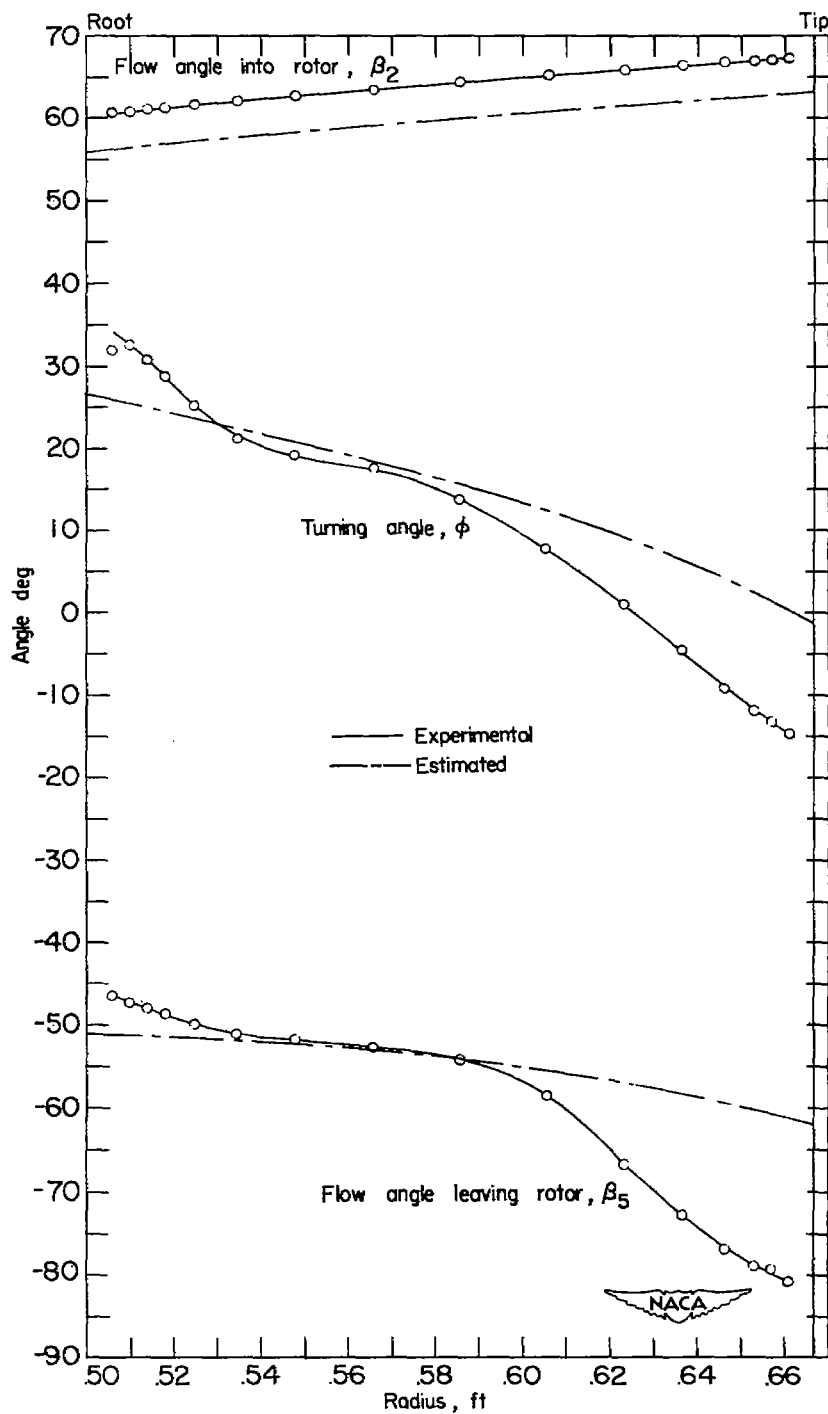
(a) Pressure-ratio distribution.

Figure 13.- Radial variation of compressor parameters at an equivalent design tip speed of 730 fps in Freon-12 without guide vanes.



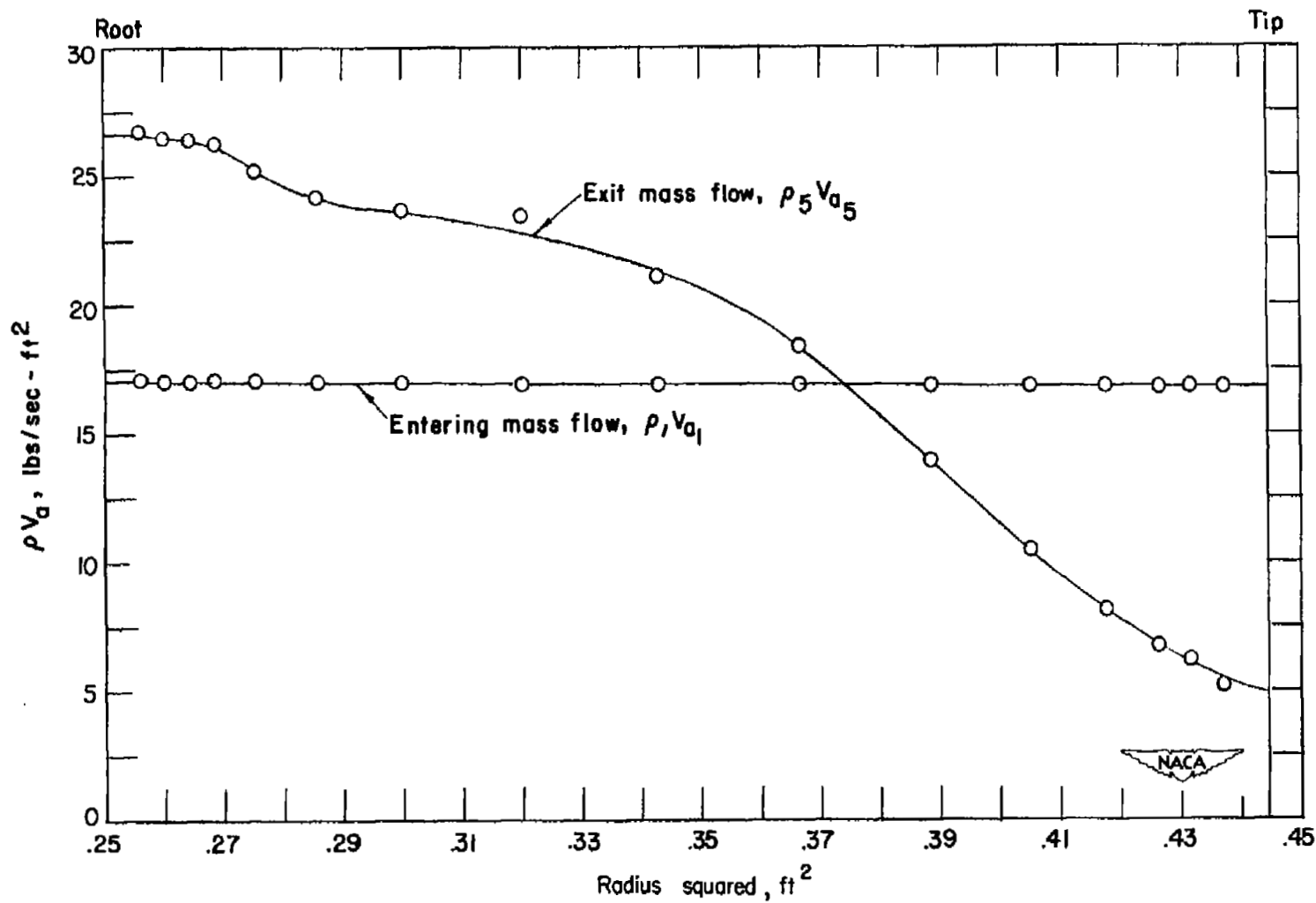
(b) Mach number distributions.

Figure 13.- Continued.



(c) Angle distribution.

Figure 13.- Continued.



(d) Mass-flow distribution. $P_o = 462.0$ lb/sq ft; $T_o = 523.9^\circ$ R.

Figure 13.- Concluded.

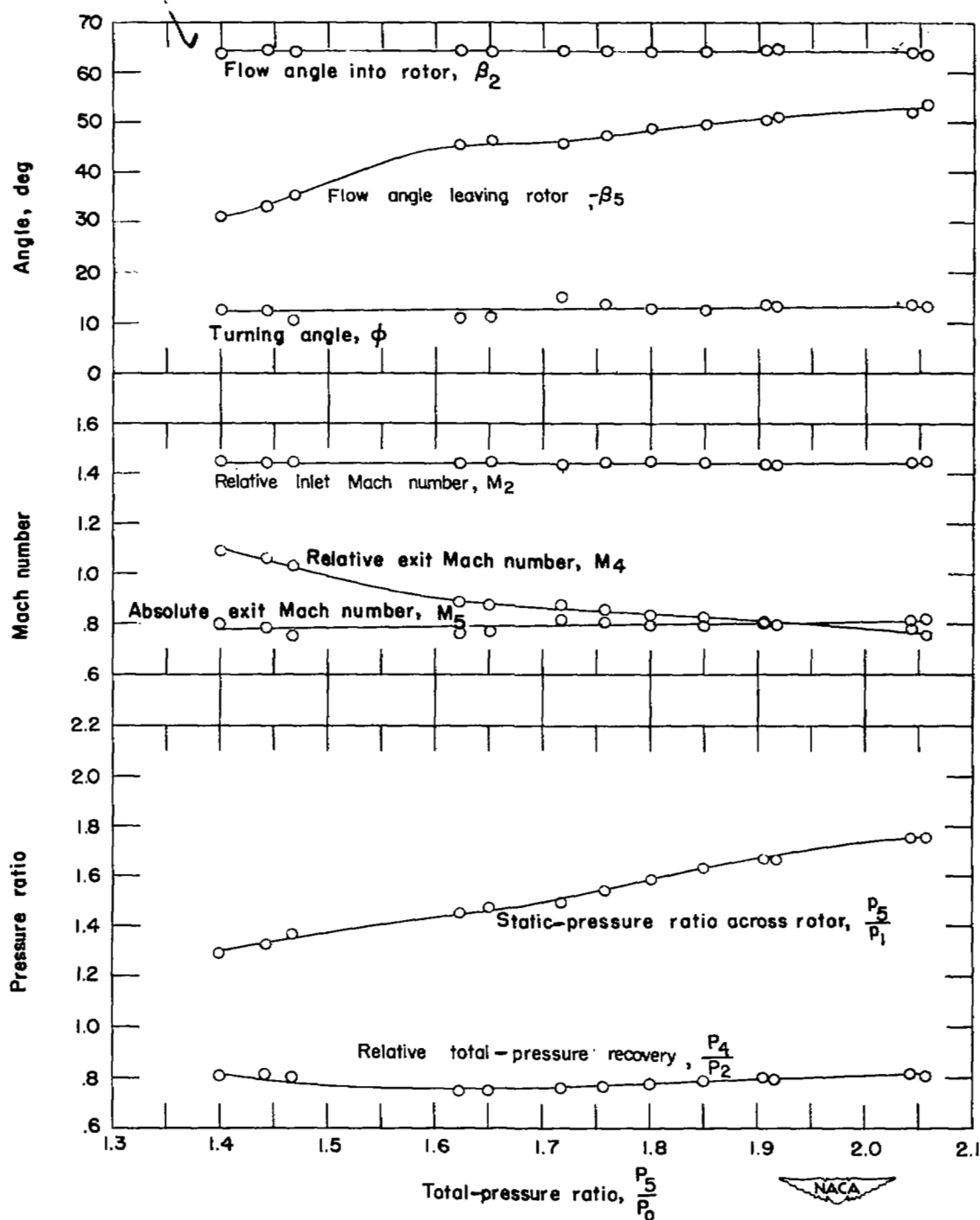


Figure 14.- Effect of throttle on compressor parameters at mean radius at an equivalent design tip speed of 730 fps in Freon-12 without guide vanes.

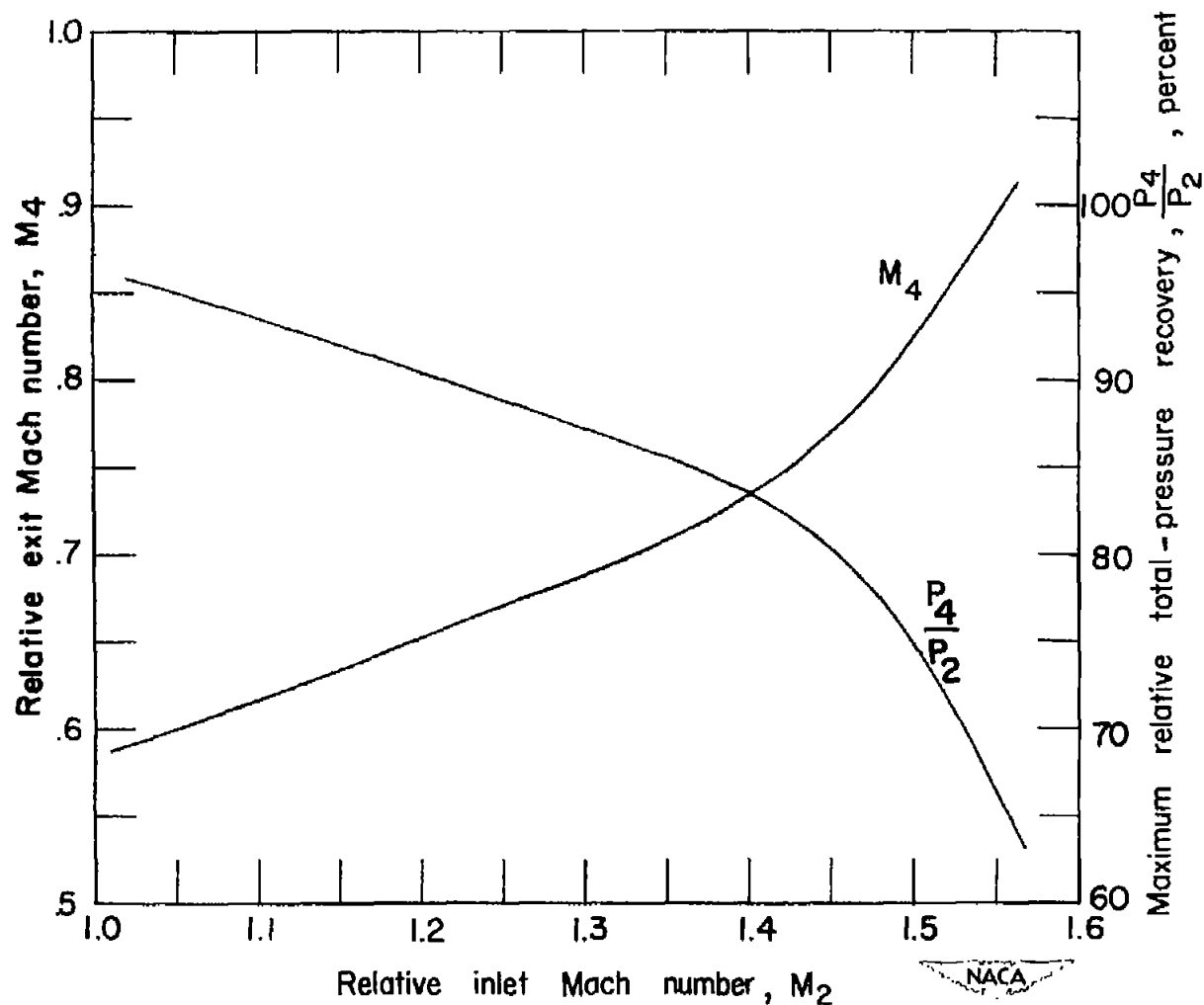
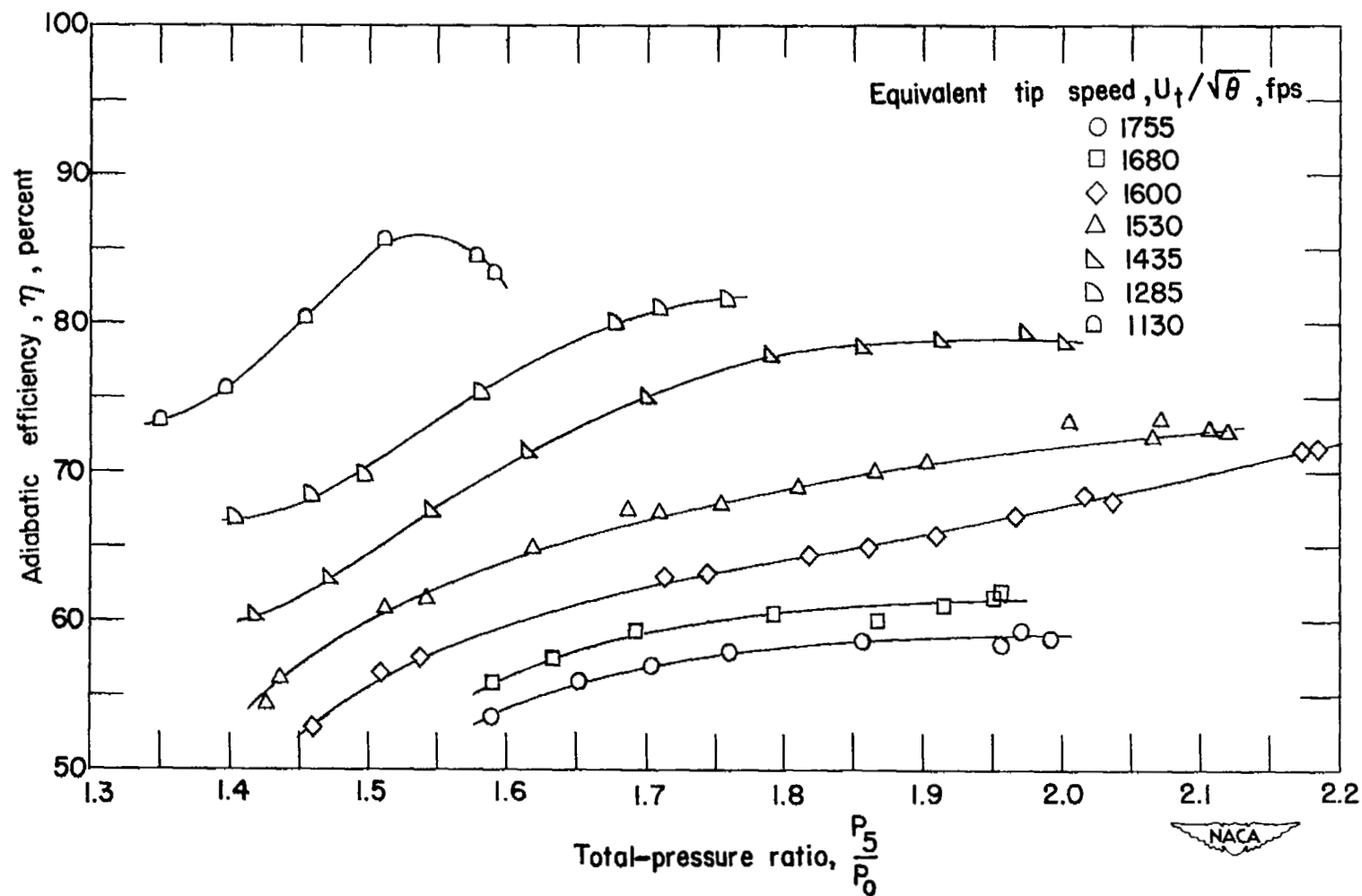
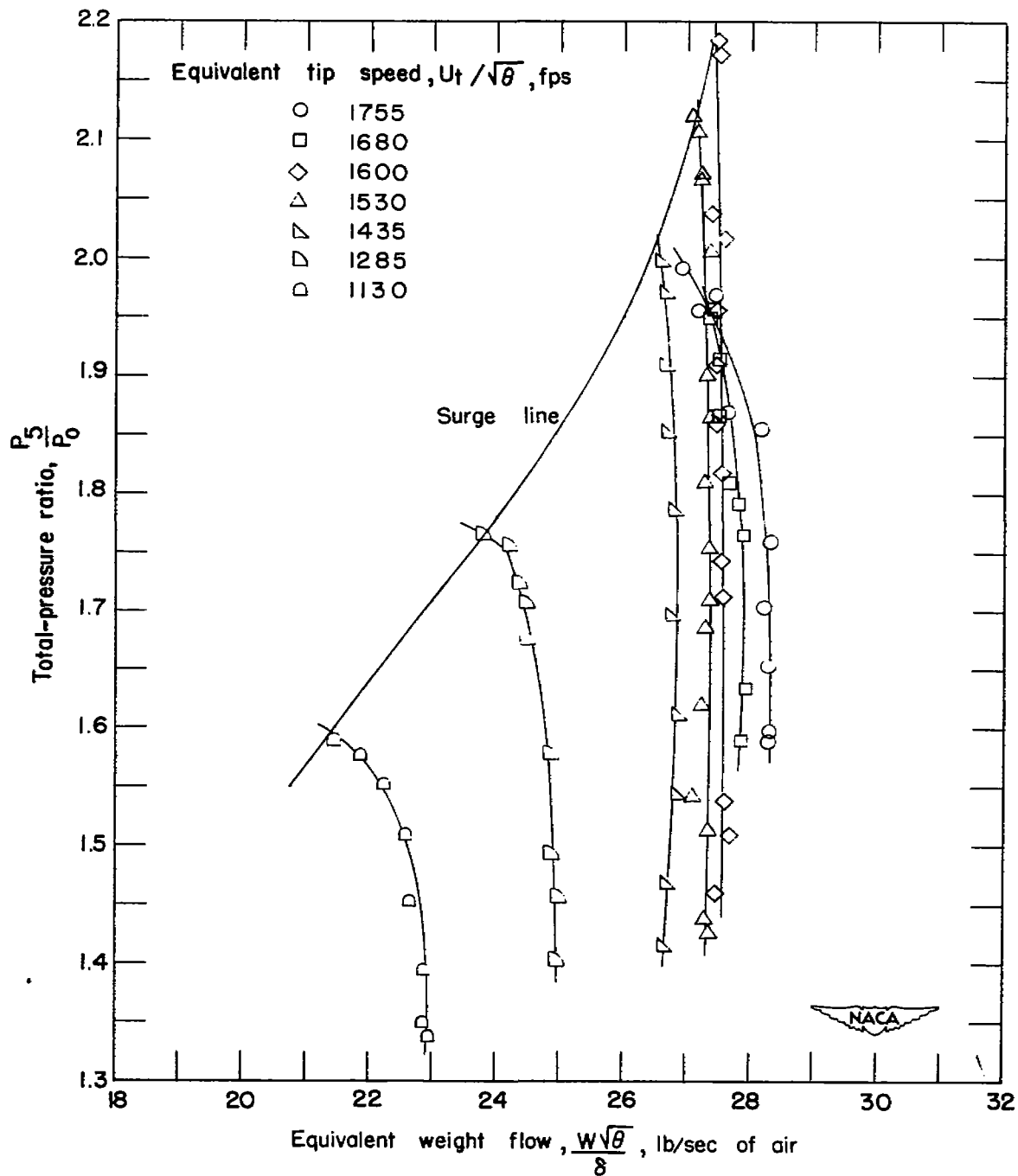


Figure 15.- Variation of relative exit Mach number and maximum relative total-pressure recovery with relative inlet Mach number measured at mean radius (without guide vanes).



(a) Total-pressure ratio against efficiency.

Figure 16.- Rotor characteristics without guide vanes. Results are converted to air.



(b) Total-pressure ratio against weight flow.

Figure 16.- Concluded.

SECURITY INFORMATION

[REDACTED]



[REDACTED]

[REDACTED]